# Core level binding energies in solids from first-principles

- Introduction of XPS
- Absolute binding energies of core states
- Applications to silicene and borophene
- Outlook

TO and C.-C. Lee, Phys. Rev. Lett. 118, 026401 (2017).
C.-C. Lee et al., Phys. Rev. B 95, 115437 (2017).
C.-C. Lee et al., Phys. Rev. B 97, 075430 (2018).

Taisuke Ozaki (ISSP, Univ. of Tokyo)

The Summer School on DFT: Theories and Practical Aspects, July 2-6, 2018, ISSP

# X-ray photoemission spectroscopy(XPS)

- Information of chemical composition, surface structure, surface adsorbates.
- XPS with synchrotron radiation extends its usefulness, e.g., satellite analysis, core level vibrational fine structure, XPS circular dichroism, spin-resolved XPS, and XPS holography.

We have developed a general method to calculate absolute binding energies of core levels in solids with the following features:

- applicable to insulators and metals
- accessible to absolute binding energies
- screening of core and valence electrons on the same footing
- SCF treatment of spin-orbit coupling
- exchange interaction between core and valence states
- geometry optimization with a core hole state

# XPS experiments

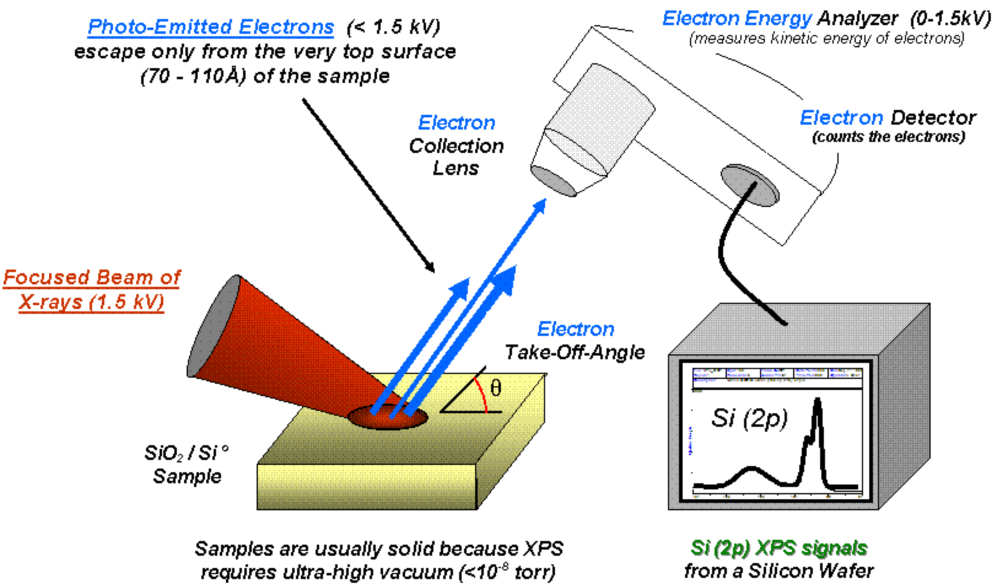

https://en.wikipedia.org/wiki/X-ray_photoelectron_spectroscopy

## Appearance of XPS equipment

In general, XPS requires high vacuum (P ~ $10^{-8}$ millibar) or ultra-high vacuum (UHV; P < $10^{-9}$ millibar) conditions.

# Basic physics in X-ray photoelectron spectroscopy (XPS)

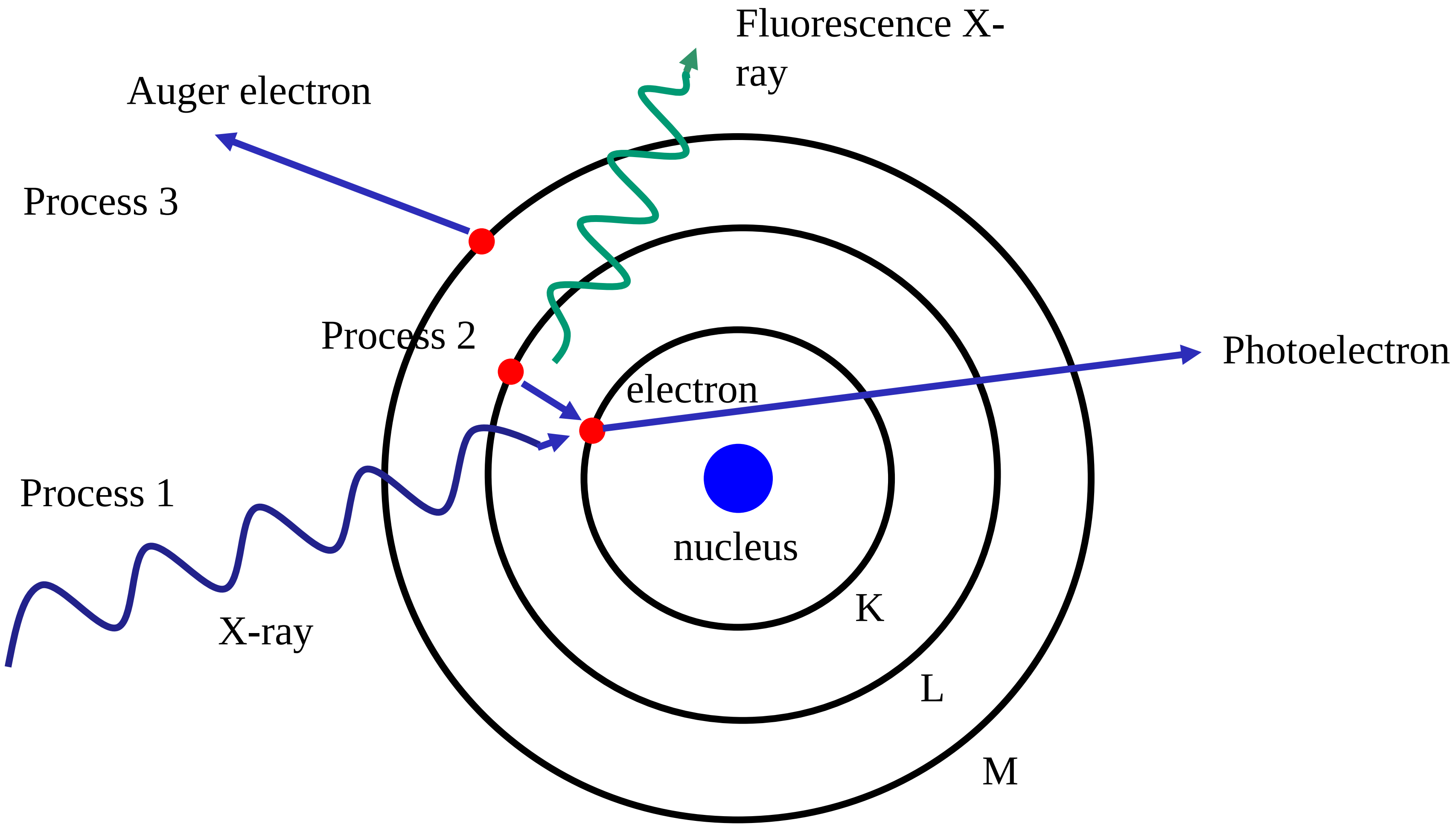

Escape time of photoelectron seems to be considered around $10^{-16}$ sec., resulting in relaxation of atomic structure would be ignored.

# Surface sensitivity

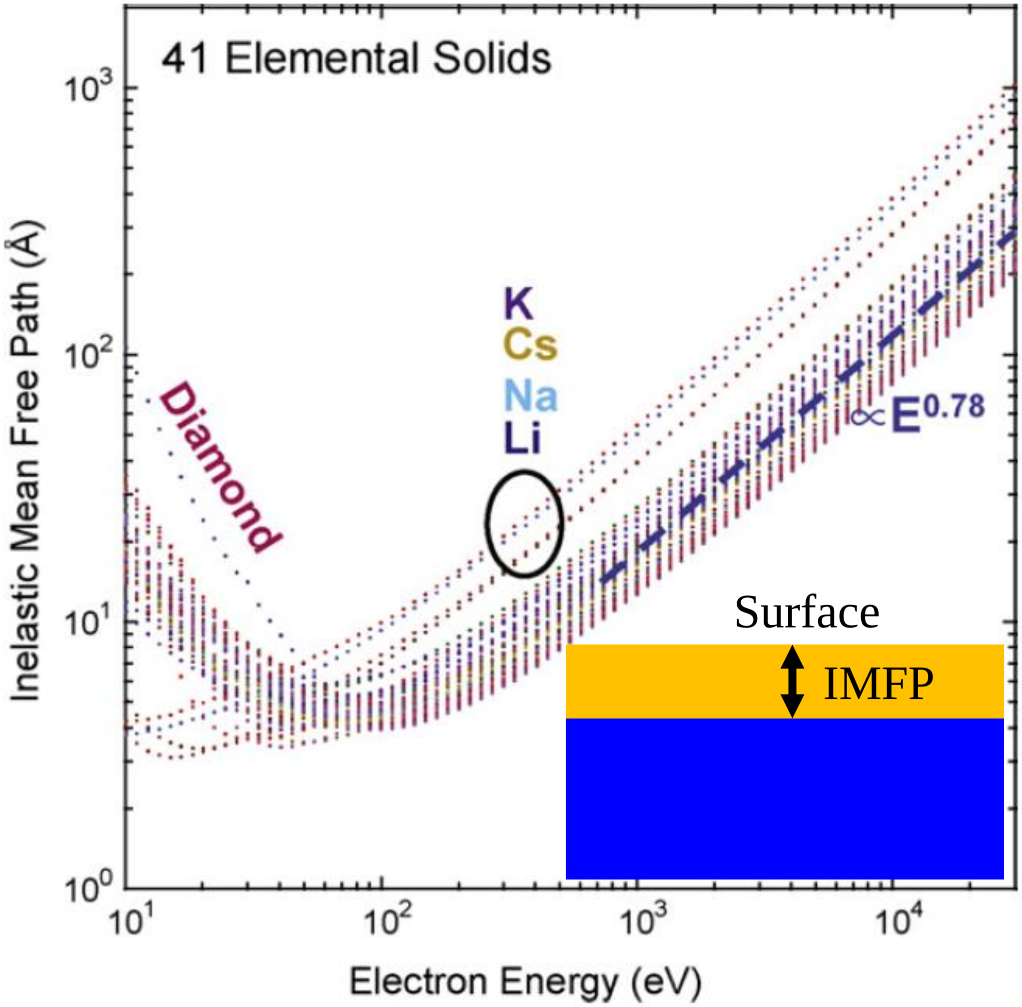

C.S. Fadley, Journal of Electron Spectroscopy and Related Phenomena 178-179, 2 (2010).

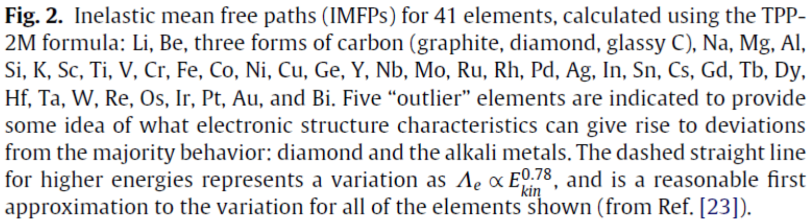
**Fig. 2.** Inelastic mean free paths (IMFPs) for 41 elements, calculated using the TPP-2M formula: Li, Be, three forms of carbon (graphite, diamond, glassy C), Na, Mg, Al, Si, K, Sc, Ti, V, Cr, Fe, Co, Ni, Cu, Ge, Y, Nb, Mo, Ru, Rh, Pd, Ag, In, Sn, Cs, Gd, Tb, Dy, Hf, Ta, W, Re, Os, Ir, Pt, Au, and Bi. Five "outlier" elements are indicated to provide some idea of what electronic structure characteristics can give rise to deviations from the majority behavior: diamond and the alkali metals. The dashed straight line for higher energies represents a variation as $\Lambda_e \propto E_{kin}^{0.78}$, and is a reasonable first approximation to the variation for all of the elements shown (from Ref. [23]).

- Inelastic Mean Free Path (IMFP) of photo excited electron for 41 elemental solids is shown the left figure.
- In case of the widely used aluminum K-alpha X-ray having 1486.7 eV, the IMFP is found to be 15 ~ 100 Å.
- On the other hand, when X-rays generated by synchrotron radiation is utilized, which have energy up to 15 keV, the IMFP can be more than 100 Å.

# Element specific measurement

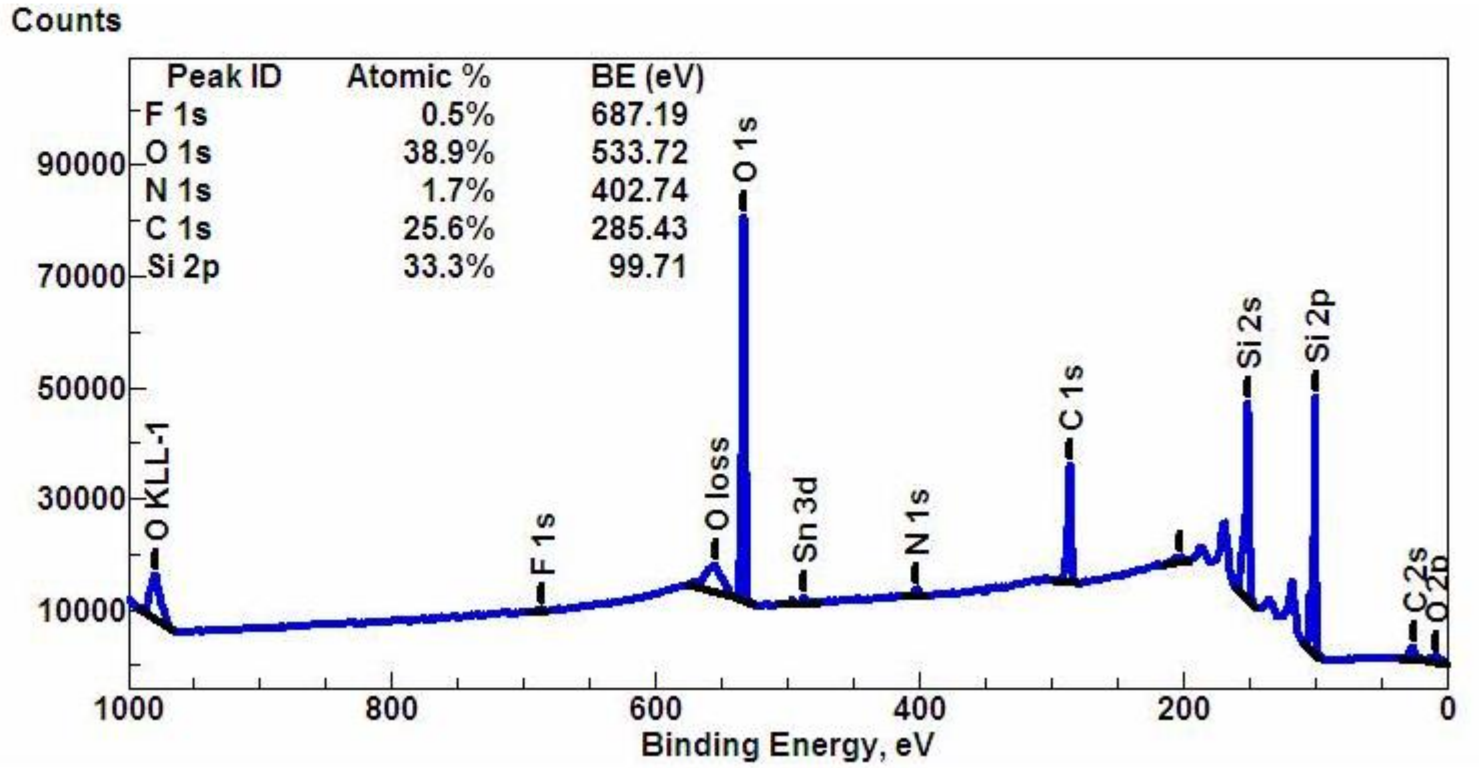

- The binding energy of each core level in each element is specific, and by this reason one can identify element and composition in a material under investigation by a wide scan mode, while hydrogen and helium cannot be identified because of low binding energies overlapping to other valence states.
- The database which is a huge collection of experimental data measured by XPS is available at http://srdata.nist.gov/xps/Default.aspx

https://en.wikipedia.org/wiki/X-ray_photoelectron_spectroscopy

# Physical origins of multiple splitting in XPS

The absolute binding energies of core electrons in solids split due to the following intrinsic physical origins:

- Chemical shift (chemical environment)
- Spin-orbit splitting
- Magnetic exchange interaction
- Chemical potential shift

# Chemical environment

- The binding energy shifts depending on its chemical environment. The amount of shift is primary determined by its charge state, known to be **initial state effect**.
- After creating the core hole, the screening of the core hole is also an important factor to determine chemical shift, known to be **final state effect**.

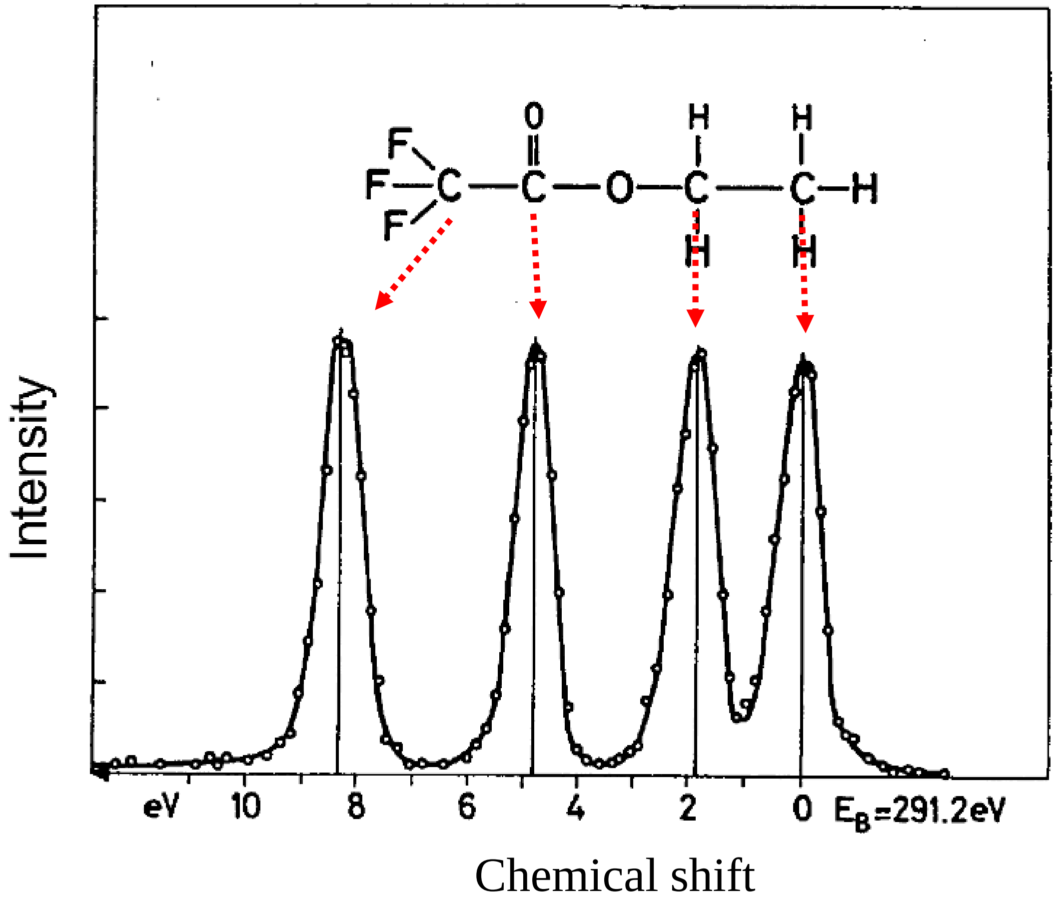

“PHOTOEMISSION
SPECTROSCOPY
Fundamental Aspects”
by Giovanni Stefani

# Spin-orbit splitting

In addition to the chemical shift, there are other multiplet splittings.

## Spin-orbit coupling of core level

- Due to the strong SOC of core level states, the binding energy is split into two levels.
- The intensity ratio is 2l: 2(l+1) for l-1/2 and l+1/2, respectively.

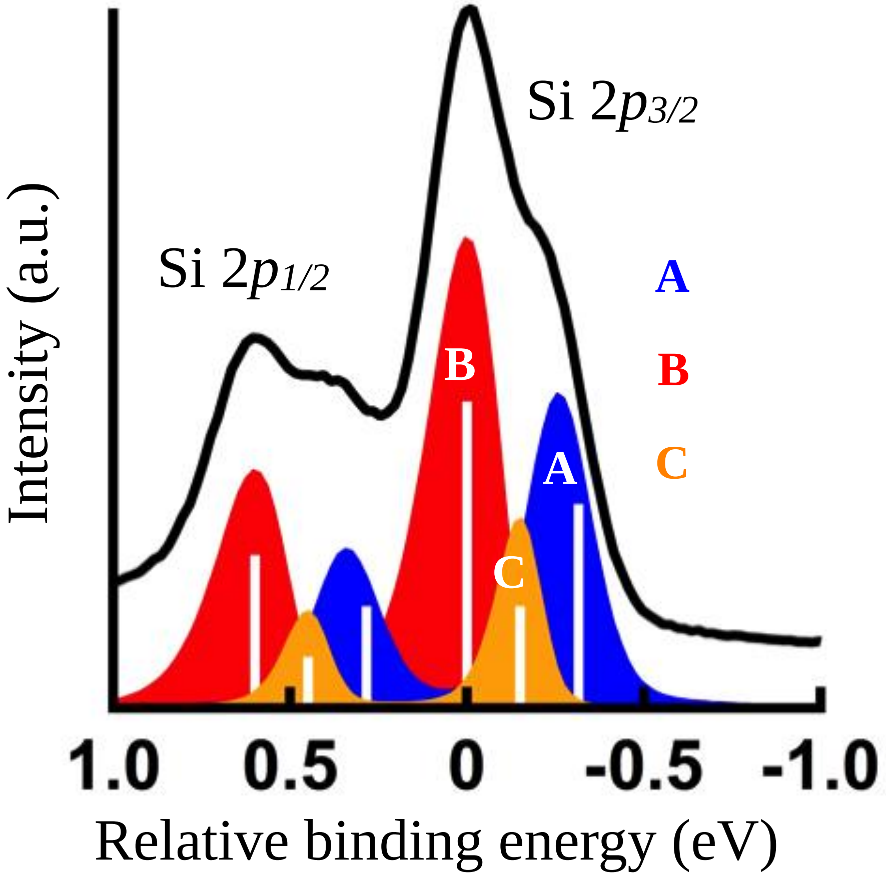

A. Fleurence et al., PRL 108, 245501 (2012).

Silicene on $ZrB_2$ surface

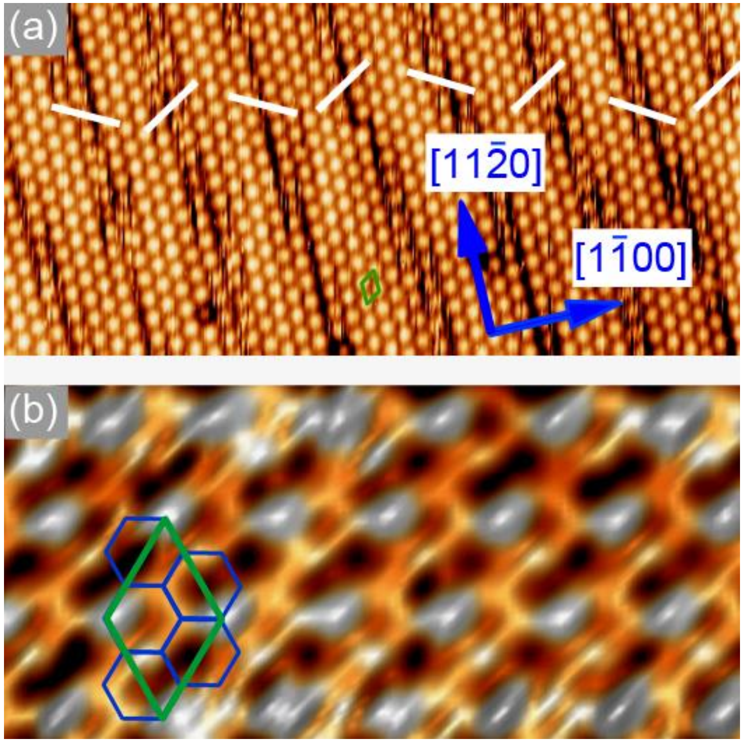

# Core level multiple splitting: Exchange interaction

## Exchange interaction between core and valence electrons

- After creation of core hole, the remaining core electron is spin polarized.
- If the valence electron is spin polarized in the initial state, there must be an exchange interaction between the remaining core electron and valence electrons even in the final state.
- The exchange interaction results in multiplet splitting.

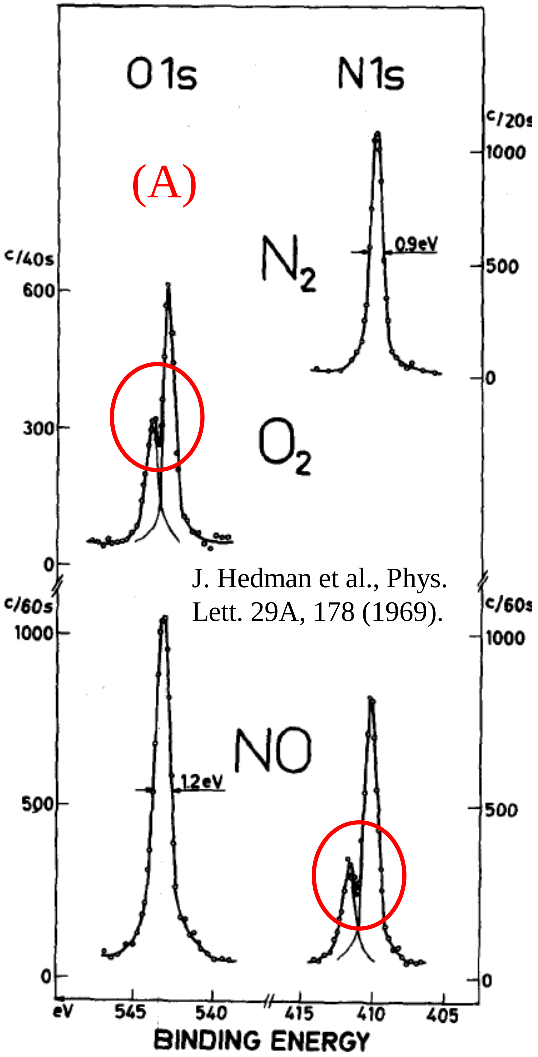

(A)

J. Hedman et al., Phys. Lett. 29A, 178 (1969).

Fig. 1. ESCA spectra of core electron levels in $N_2$, $O_2$, and NO. Paramagnetic splitting is observed for the 1s levels in the $O_2$ and NO molecules.

- The left figure (A) shows that the 1s binding energy of oxygen and nitrogen atom splits in magnetic molecules $O_2$ and NO, respectively, while no splitting is observed in $N_2$ being a non-magnetic molecule.
- The right figure (B) shows the splitting of 3s binding energy of Mn atom in manganese compounds.

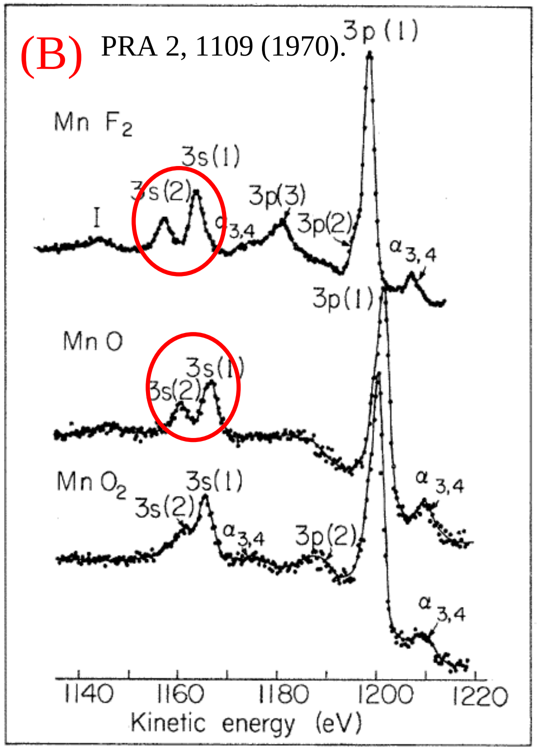

(B) PRA 2, 1109 (1970).

FIG. 1. Photoelectron spectra from $MnF_2$, MnO, and $MnO_2$ in the kinetic-energy region corresponding to ejection of Mn 3*s* and 3*p* electrons by Mg *Kα* x rays.

# Shift of chemical potential in semi-conductors and insulators

The chemical potential in gapped systems varies sensitively depending on impurity, vacancy, surface structures, and adsorbate.

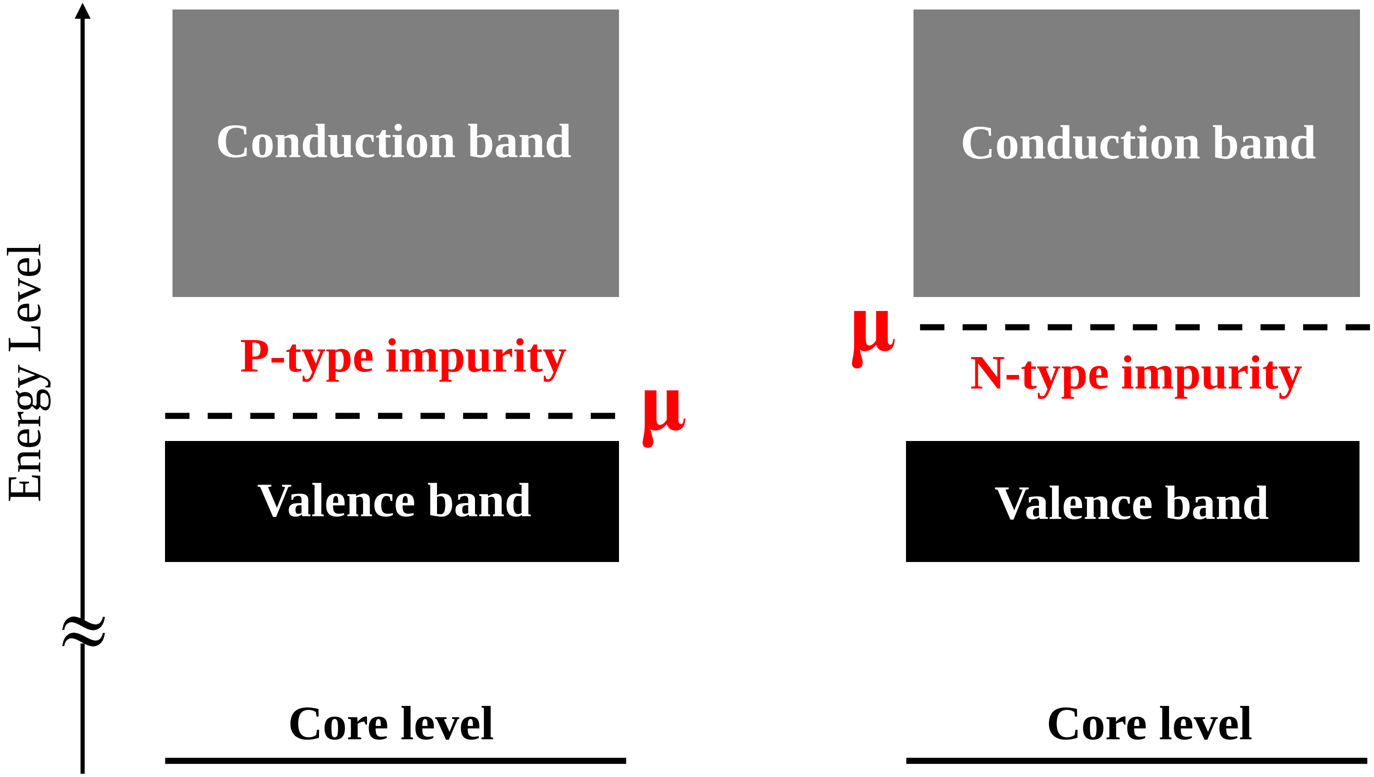

Severely speaking, we need to take account of the effect explicitly by considering realistic models which reflect experimental situations.

# Energy conservation in XPS

$$E_{\mathrm{i}}(N) + h\nu = E_{\mathrm{f}}(N-1) + V_{\mathrm{spec}} + K_{\mathrm{spec}}$$

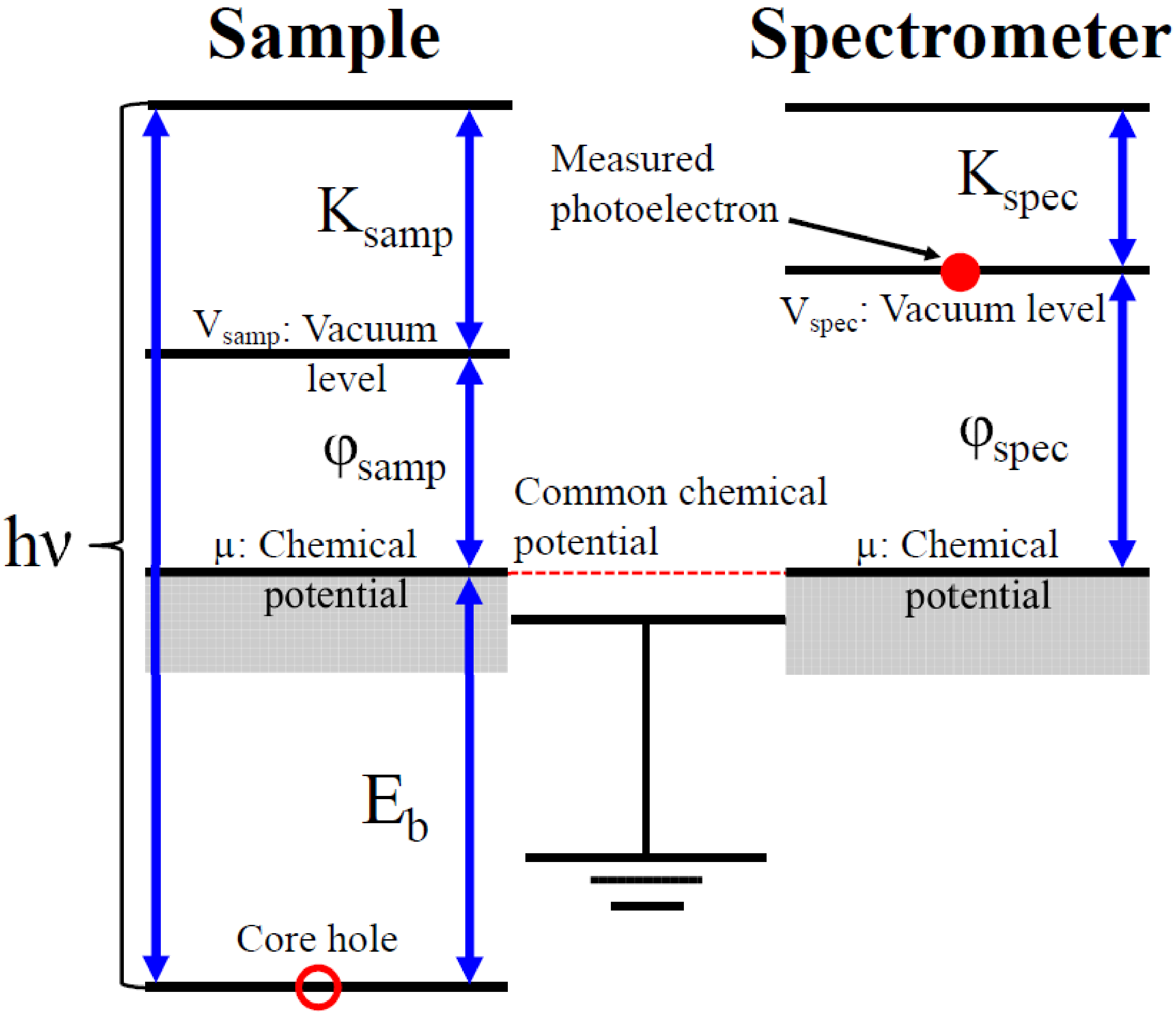

# Core level binding energies in XPS #1

$$E_{\mathrm{i}}(N) + h\nu = E_{\mathrm{f}}(N-1) + V_{\mathrm{spec}} + K_{\mathrm{spec}}$$

Using a relation: $V_{\mathrm{spec}} = \mu + \varphi_{\mathrm{spec}}$ we have

$$E_{\mathrm{b}} = h\nu - K_{\mathrm{spec}} - \phi_{\mathrm{spec}} = E_{\mathrm{f}}(N-1) - E_{\mathrm{i}}(N) + \mu$$

The experimental chemical potential can be transformed as

$$E_{\mathrm{b}} = E_{\mathrm{f}}^{(0)}(N-1) + (N-1)\Delta\mu - \left(E_{\mathrm{i}}^{(0)}(N) + N\Delta\mu\right) + \mu_{0} + \Delta\mu$$

A general formula of core level binding is given by

$$\boxed{E_{\mathrm{b}} = E_{\mathrm{f}}^{(0)}(N-1) - E_{\mathrm{i}}^{(0)}(N) + \mu_{0}}$$

This is common for metals and insulators.

# Core level binding energies in XPS #2

For metals, the Janak theorem simplifies the formula:

$$E_{\mathrm{f}}^{(0)}(N-1)-E_{\mathrm{f}}^{(0)}(N)=\int dn\partial E_{\mathrm{f}}^{(0)}/\partial n=-\mu_0$$

$$E_{\mathrm{b}}=E_{\mathrm{f}}^{(0)}(N)-E_{\mathrm{i}}^{(0)}(N)$$

The formulae of core level binding energies are summarized as

| | |
|---|---|
| Solids (gapped systems, metals) | $E_{\mathrm{b}}=E_{\mathrm{f}}^{(0)}(N-1)-E_{\mathrm{i}}^{(0)}(N)+\mu_0$ |
| Metals | $E_{\mathrm{b}}=E_{\mathrm{f}}^{(0)}(N)-E_{\mathrm{i}}^{(0)}(N)$ |
| Gases | $E_{\mathrm{b}}=E_{\mathrm{f}}^{(0)}(N-1)-E_{\mathrm{i}}^{(0)}(N)$ |

# Calculations: core level binding energy

Within DFT, there are at least three ways to to calculate the binding energy of a core state as summarized below:

1. **Initial state theory**

   Simply the density of states is taken into account

2. **Core-hole pseudopotential method**

   Full initial and semi-final state effects are taken into account

   E. Pehlke and M. Scheffler, PRL 71 2338 (1993).

3. **Core-hole SCF method**

   The initial and final state effects are fully taken into account on the same footing.

The method 3 can be regarded as the most accurate scheme among the three methods, and enables us to obtain the absolute value of binding energy and splitting due to spin-orbit coupling and spin interaction between the remaining core state and spin-polarized valence states.

# Constraint DFT with a penalty functional

$$E_{\mathrm{f}} = E_{\mathrm{DFT}} + E_{\mathrm{p}}$$

Fully relativistic PPs and two-component spinor are employed.

$E_{\mathrm{DFT}}$ is a conventional functional of DFT, and $E_{\mathrm{p}}$ is a penalty functional defined by

$$E_{\mathrm{p}} = \frac{1}{V_{\mathrm{B}}} \int dk^3 \sum_{\mu} f_{\mu}^{(\mathbf{k})} \langle \psi_{\mu}^{(\mathbf{k})} | \hat{P} | \psi_{\mu}^{(\mathbf{k})} \rangle$$

$$\hat{P} = \left| R\Phi_J^M \right\rangle \Delta \left\langle R\Phi_J^M \right|$$

R: radial function of the core level

The projector is given by a solution of Dirac eq. for atoms.

$$J = l + \frac{1}{2}, M = m + \frac{1}{2}$$

$$|\Phi_J^M\rangle = \left( \frac{l+m+1}{2l+1} \right)^{\frac{1}{2}} |Y_l^m\rangle + \left( \frac{l-m}{2l+1} \right)^{\frac{1}{2}} |Y_l^{m+1}\rangle$$

$$J = l - \frac{1}{2}, M = m - \frac{1}{2}$$

$$|\Phi_J^M\rangle = \left( \frac{l-m+1}{2l+1} \right)^{\frac{1}{2}} |Y_l^{m-1}\rangle + \left( \frac{l+m}{2l+1} \right)^{\frac{1}{2}} |Y_l^m\rangle$$

# Kohn-Sham eq. with a penalty operator

By variationally differentiating the penalty functional $E_f$, we obtain the following the KS equation.

$$\left(\hat{T} + V_{\mathrm{eff}} + \hat{P}\right) | \psi_{\mu}^{(\mathbf{k})} \rangle = \varepsilon_{\mu}^{(\mathbf{k})} | \psi_{\mu}^{(\mathbf{k})} \rangle$$

## Features of the method

- applicable to insulators and metals
- accessible to absolute binding energies
- screening of core and valence electrons on the same footing
- SCF treatment of spin-orbit coupling
- exchange interaction between core and valence states
- geometry optimization with a core hole state

# Elimination of inter-core hole interaction

$$\rho_{\mathrm{f}}(\mathbf{r}) = \rho_{\mathrm{i}}(\mathbf{r}) + \Delta\rho(\mathbf{r})$$

$$\Delta\rho(\mathbf{r}) = \rho_f(\mathbf{r}) - \rho_i(\mathbf{r})$$

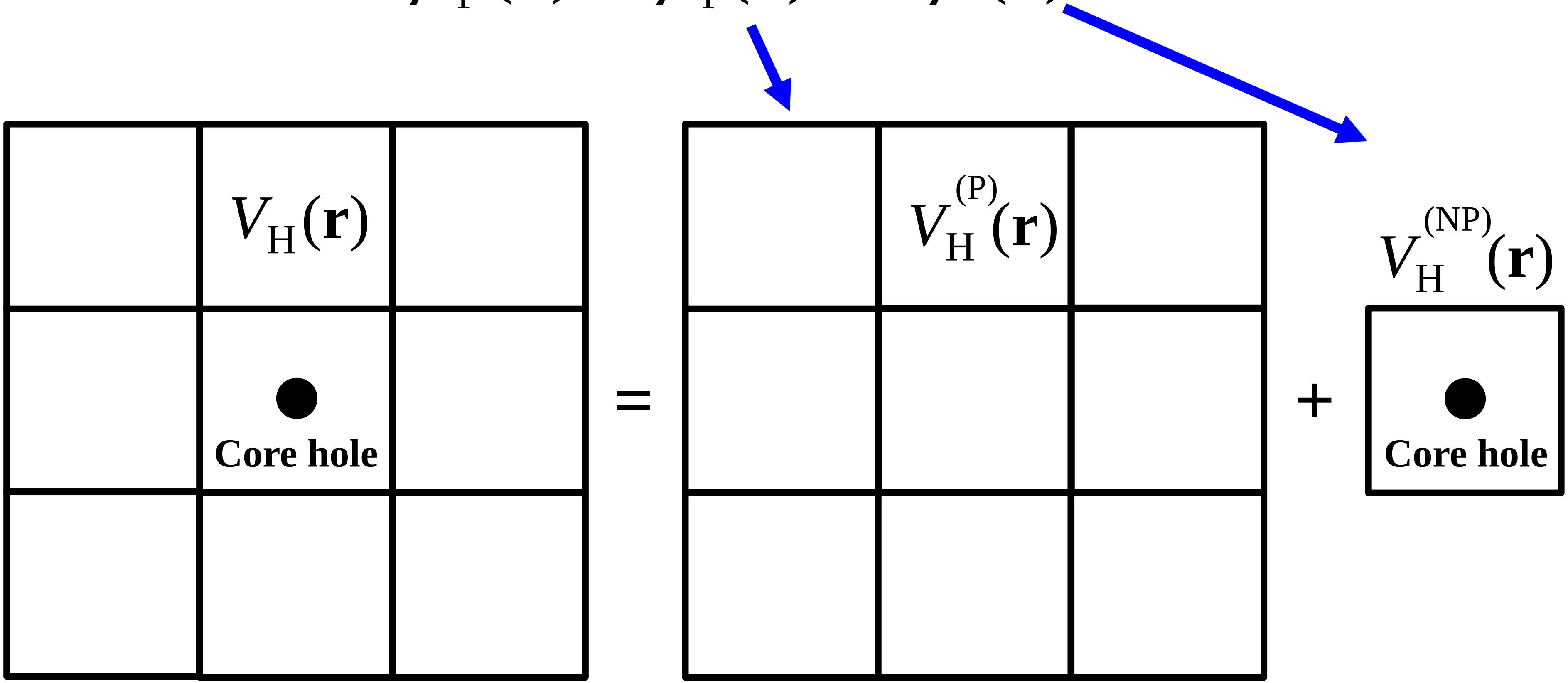

- Periodic Hartree potential is calculated by charge density of the initial state.
- Potential by induced charge is calculated by an exact Coulomb cutoff method.

# Exact Coulomb cutoff method #1

If the charge induced by a core hole localizes within a radius of R, we can set $R_c=2R$, and the cutoff condition becomes $2R_c<L$ to eliminate the inter-core hole interaction.

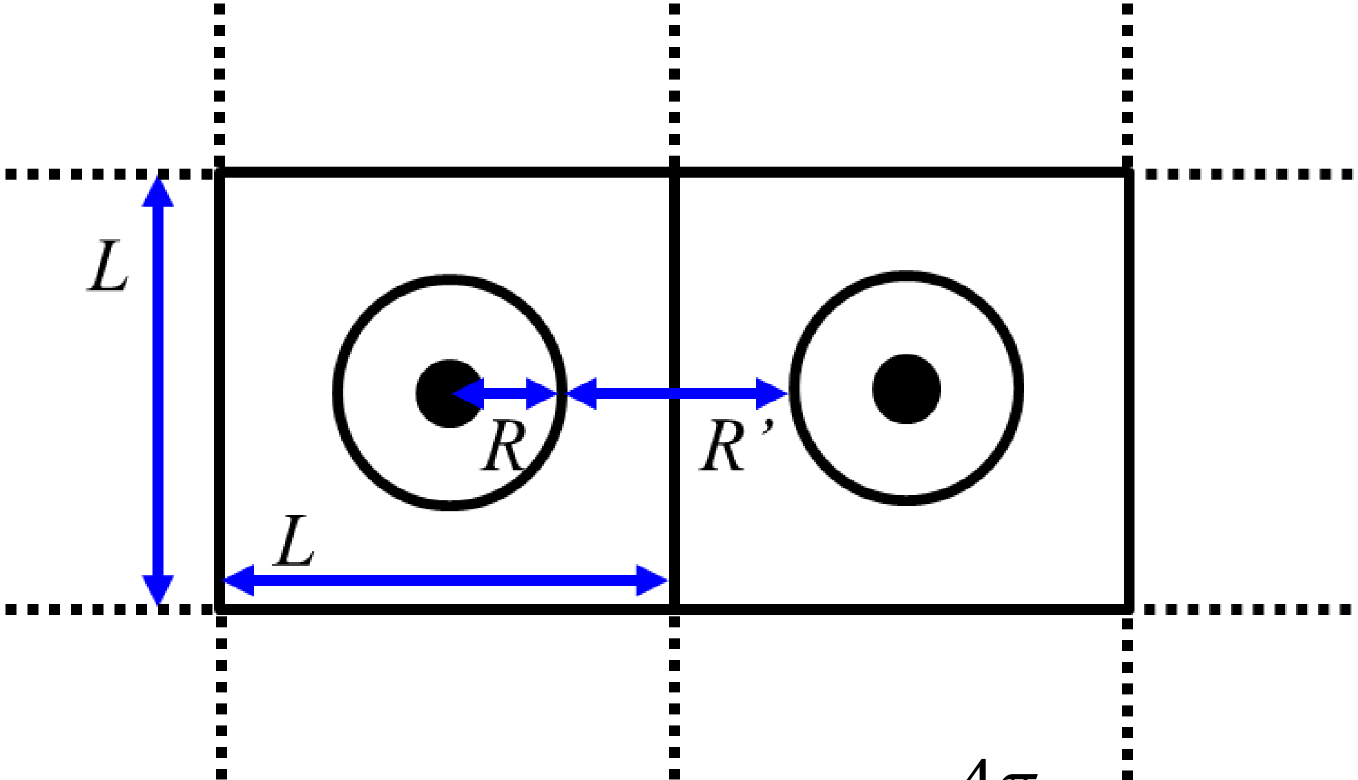

$$v_{\mathrm{H}}(r)=\sum_{\mathbf{G}}\tilde{n}(\mathbf{G})\tilde{v}(\mathbf{G})\mathrm{e}^{i\mathbf{G}\bullet r} \qquad \tilde{v}(\mathbf{G})=\frac{4\pi}{G^2}(1-\cos GR_{\mathrm{c}})$$

Jarvis et al., PRB 56, 14972 (1997).

# Exact Coulomb cutoff #2

$$v_{\mathrm{H}}(r) = \int dr' n(r') v(|r - r'|) \quad \cdots(1)$$

$$n(r) = \sum_{\mathbf{G}} \tilde{n}(\mathbf{G})\, \mathrm{e}^{i\mathbf{G}\bullet r} \quad \cdots(2) \qquad v(r) = \sum_{\mathbf{G}} \tilde{v}(\mathbf{G})\, \mathrm{e}^{i\mathbf{G}\bullet r} \quad \cdots(3)$$

By inserting (2) and (3) into (1), and performing the integration, we obtain

$$v_{\mathrm{H}}(r) = \sum_{\mathbf{G}} \tilde{n}(\mathbf{G}) \tilde{v}(\mathbf{G}) \mathrm{e}^{i\mathbf{G}\bullet r}$$

$\tilde{v}(\mathbf{G})$ is evaluated by performing the integration as

$$v(r) = \frac{1}{r} \quad \text{if r<=R}_{\mathrm{c}} \qquad \tilde{v}(\mathbf{G}) = \int_0^{R_{\mathrm{c}}} dr r^2 \int_0^{2\pi} d\phi \int_0^{\pi} d\theta \sin\theta \frac{\mathrm{e}^{i\mathbf{G}\bullet\mathbf{r}}}{r}$$

$$v(r) = 0 \quad \text{if R}_{\mathrm{c}}\text{<r} \qquad \tilde{v}(\mathbf{G}) = \frac{4\pi}{G^2}(1 - \cos GR_{\mathrm{c}})$$

C.A. Rozzi et al., PRB 73, 205119.

# Convergence w. r. t cell size

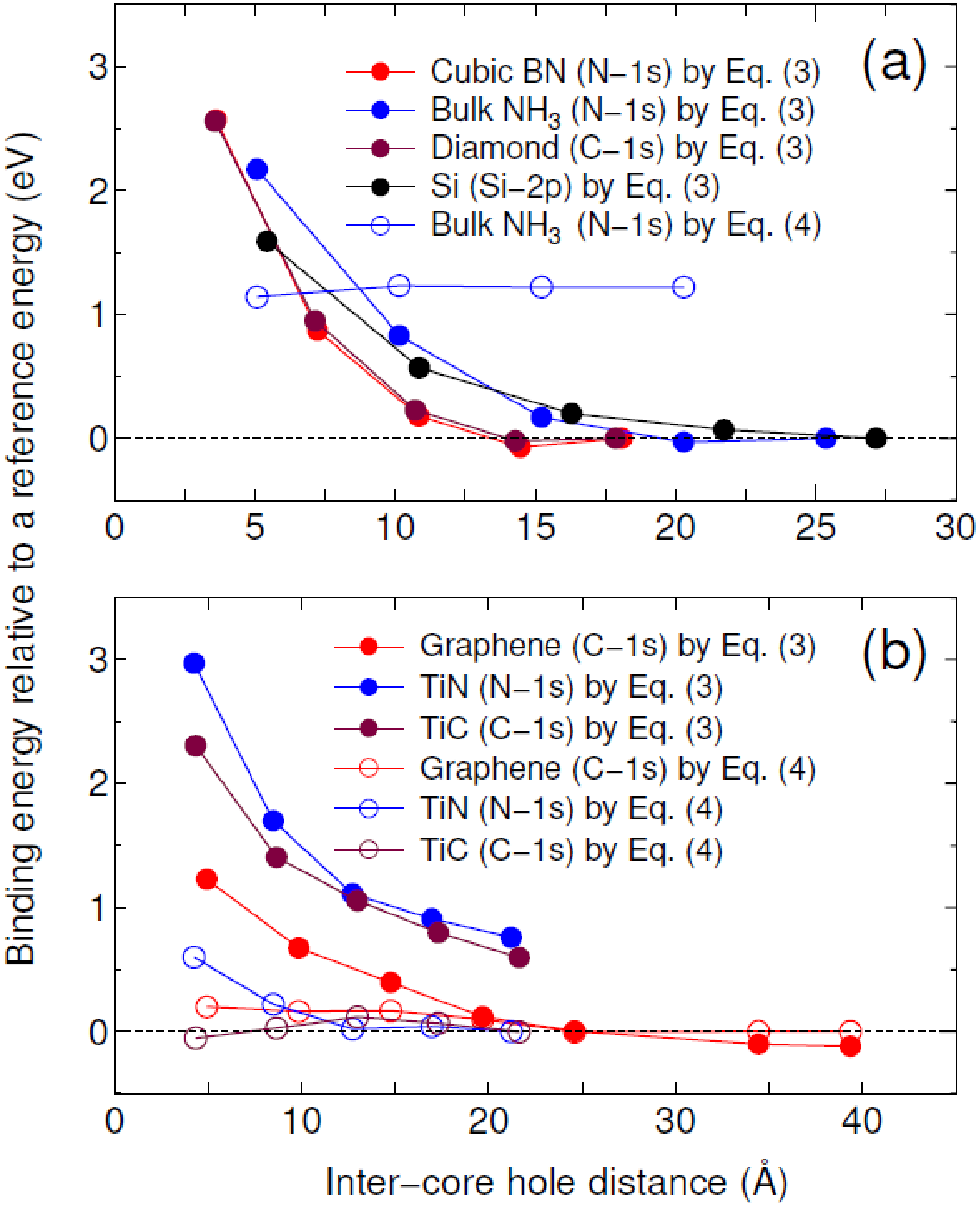

General formula

$$E_{\mathrm{b}} = E_{\mathrm{f}}^{(0)}(N-1) - E_{\mathrm{i}}^{(0)}(N) + \mu_0$$

···(3)

For metals

$$E_{\mathrm{b}} = E_{\mathrm{f}}^{(0)}(N) - E_{\mathrm{i}}^{(0)}(N)$$

···(4)

- Convergence is attainable around 15～20Å.
- The formula for metals is not applicable for gapped systems.
- Very fast convergence by Eq. (4) for metals.

# Difference charge induced by a core hole in Si

- The effective radius is about 7Å.
- The core hole is almost screened on the same Si atom.

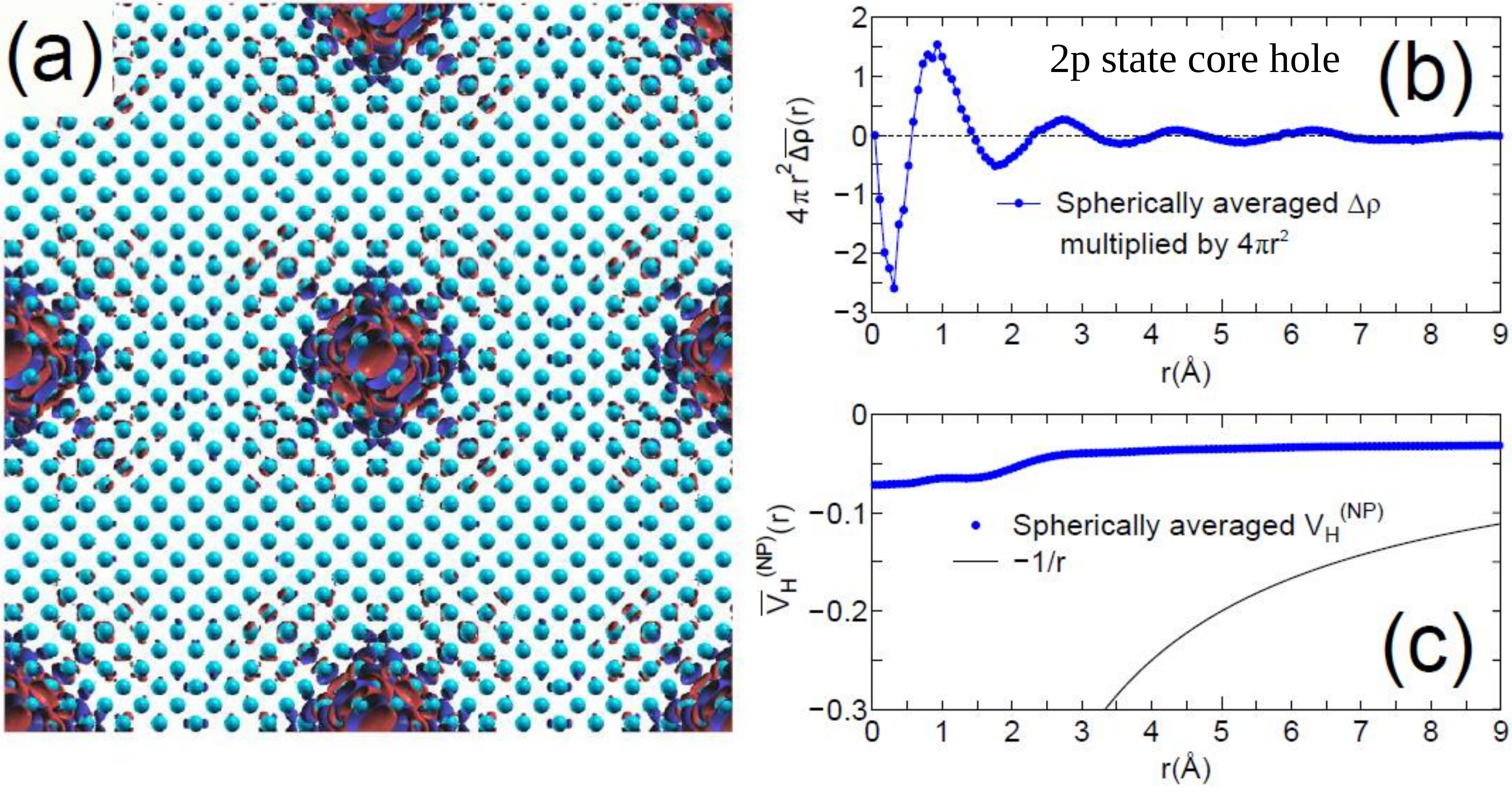

# Absolute values: Expt. vs. Calcs. for solids

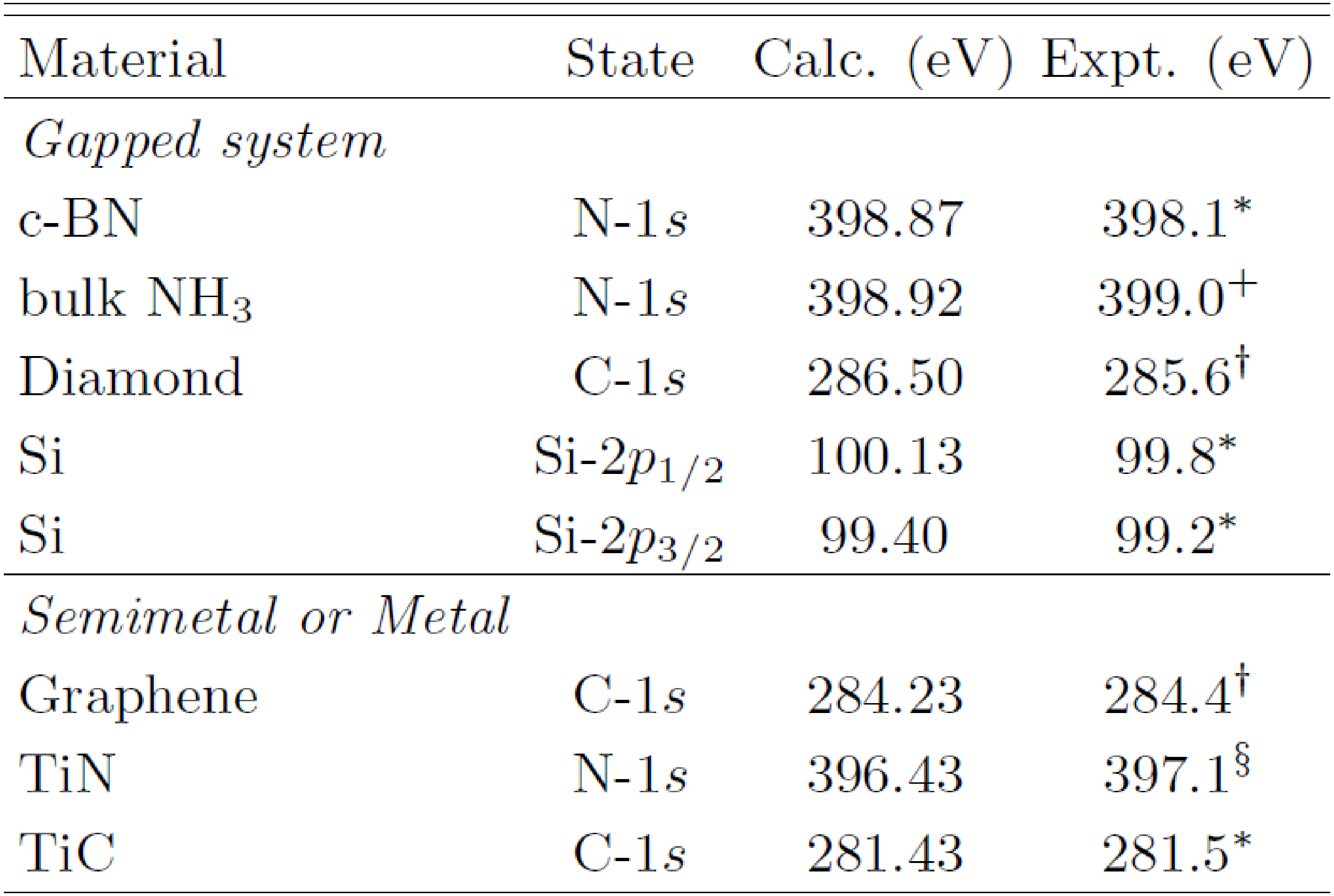

| Material | State | Calc. (eV) | Expt. (eV) |
|---|---|---|---|
| *Gapped system* | | | |
| c-BN | N-1$s$ | 398.87 | 398.1$^*$ |
| bulk $NH_3$ | N-1$s$ | 398.92 | 399.0$^+$ |
| Diamond | C-1$s$ | 286.50 | 285.6$^\dagger$ |
| Si | Si-2$p_{1/2}$ | 100.13 | 99.8$^*$ |
| Si | Si-2$p_{3/2}$ | 99.40 | 99.2$^*$ |
| *Semimetal or Metal* | | | |
| Graphene | C-1$s$ | 284.23 | 284.4$^\dagger$ |
| TiN | N-1$s$ | 396.43 | 397.1$^\S$ |
| TiC | C-1$s$ | 281.43 | 281.5$^*$ |

Mean absolute error: 0.4 eV, Mean relative error: 0.16 %

# Absolute values: Expt. vs. Calcs. for gases

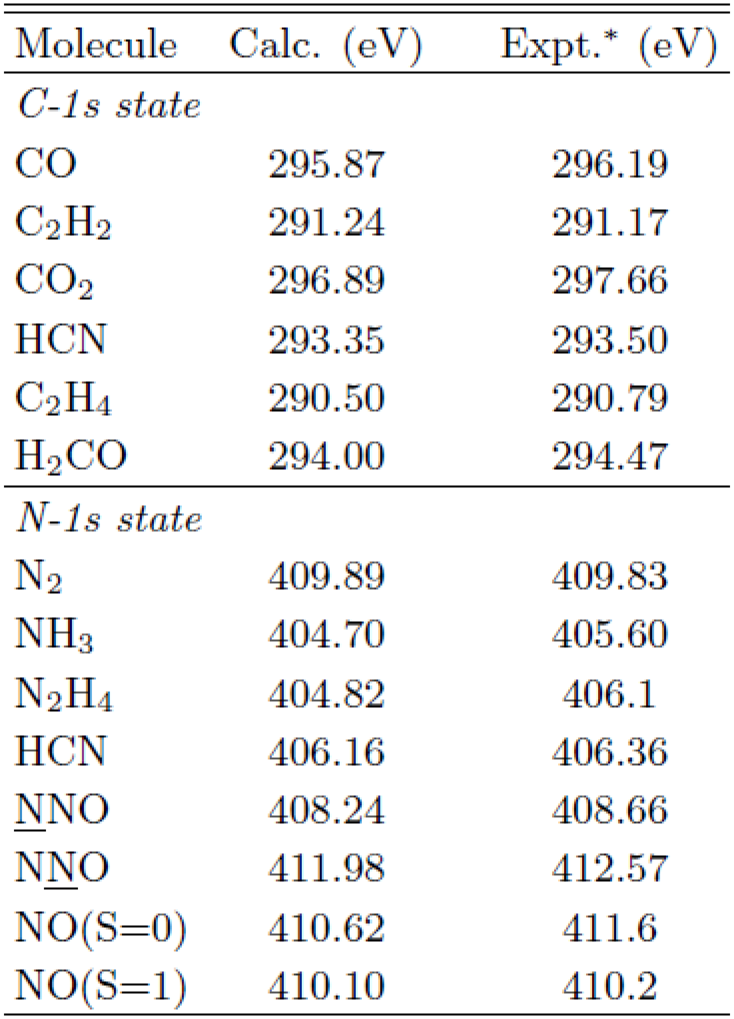

| Molecule | Calc. (eV) | Expt.* (eV) |
|---|---|---|
| *C-1s state* | | |
| CO | 295.87 | 296.19 |
| $C_2H_2$ | 291.24 | 291.17 |
| $CO_2$ | 296.89 | 297.66 |
| HCN | 293.35 | 293.50 |
| $C_2H_4$ | 290.50 | 290.79 |
| $H_2CO$ | 294.00 | 294.47 |
| *N-1s state* | | |
| $N_2$ | 409.89 | 409.83 |
| $NH_3$ | 404.70 | 405.60 |
| $N_2H_4$ | 404.82 | 406.1 |
| HCN | 406.16 | 406.36 |
| $\underline{N}NO$ | 408.24 | 408.66 |
| $N\underline{N}O$ | 411.98 | 412.57 |
| NO(S=0) | 410.62 | 411.6 |
| NO(S=1) | 410.10 | 410.2 |

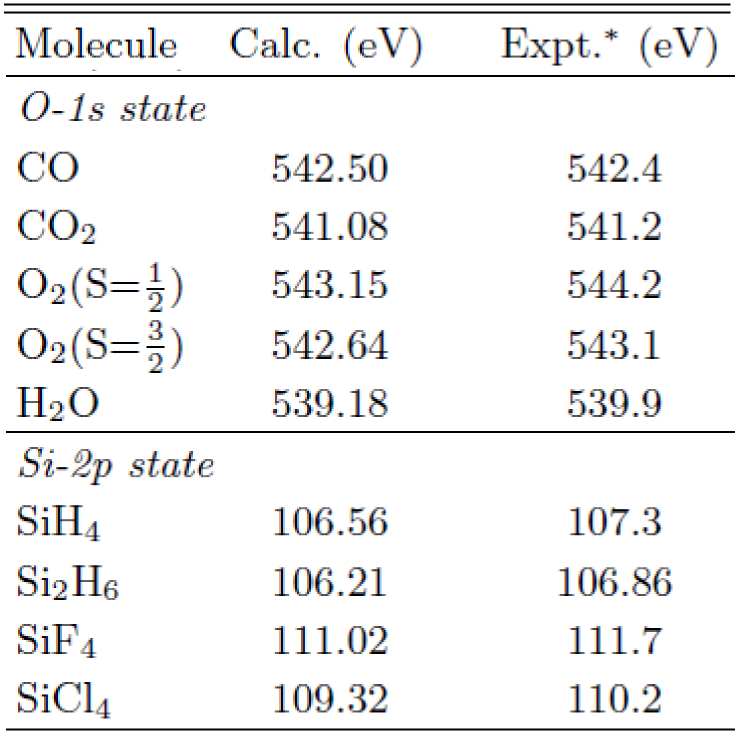

| Molecule | Calc. (eV) | Expt.* (eV) |
|---|---|---|
| *O-1s state* | | |
| CO | 542.50 | 542.4 |
| $CO_2$ | 541.08 | 541.2 |
| $O_2(S=\frac{1}{2})$ | 543.15 | 544.2 |
| $O_2(S=\frac{3}{2})$ | 542.64 | 543.1 |
| $H_2O$ | 539.18 | 539.9 |
| *Si-2p state* | | |
| $SiH_4$ | 106.56 | 107.3 |
| $Si_2H_6$ | 106.21 | 106.86 |
| $SiF_4$ | 111.02 | 111.7 |
| $SiCl_4$ | 109.32 | 110.2 |

Mean absolute error: 0.5 eV

Mean relative error: 0.22 %

# Characterization of silicene structre

PRL 108, 245501 (2012).
PRB 90, 075422 (2014).
PRB 90, 241402 (2014).
PRB 95, 115437 (2017).

# Experimental report of silicene on $ZrB_2(0001)$

Yamada-Takamura group of JAIST

$ZrB_2$ on Si(111) is a promising substrate for a photo emitting device of GaN due to the lattice matching, metallicity, and flatness. It was found that Si atoms form a super structure during CVD by probably migration and segregation of Si atoms from the Si substrate.

STM image

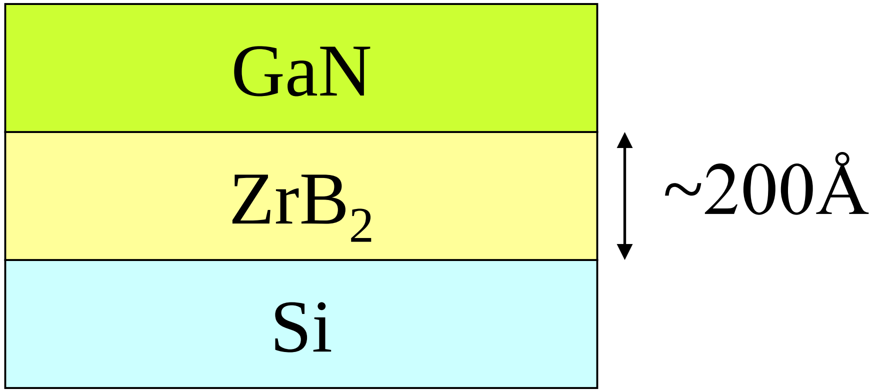
GaN

$ZrB_2$

Si

~200Å

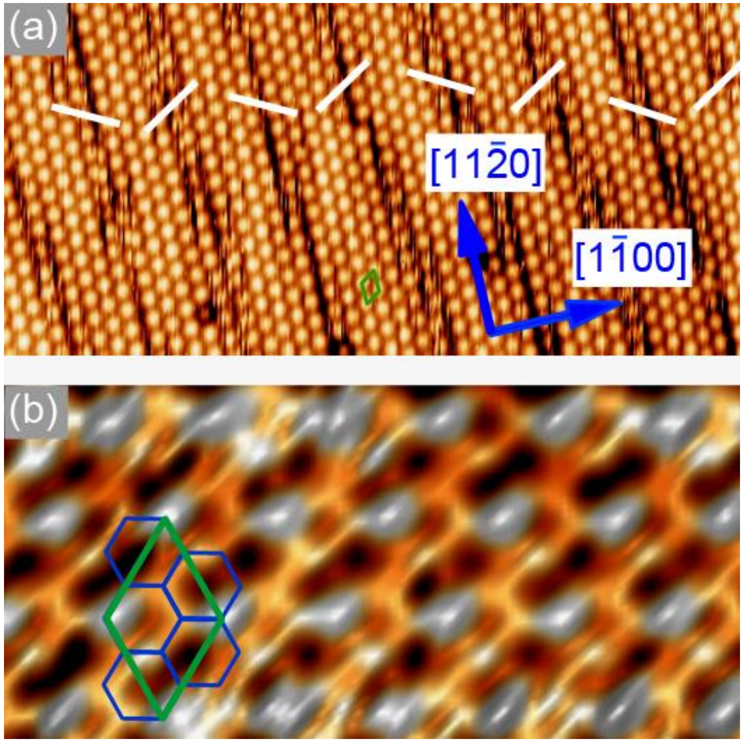

GaN(0001): a= 3.189Å

$ZrB_2(0001)$: a= 3.187Å

A. Fleurence et al., PRL 108, 245501 (2012).

# Top view of optimized structures

- Two buckled structures are obtained.
- Both the structures keep the honeycomb lattice.

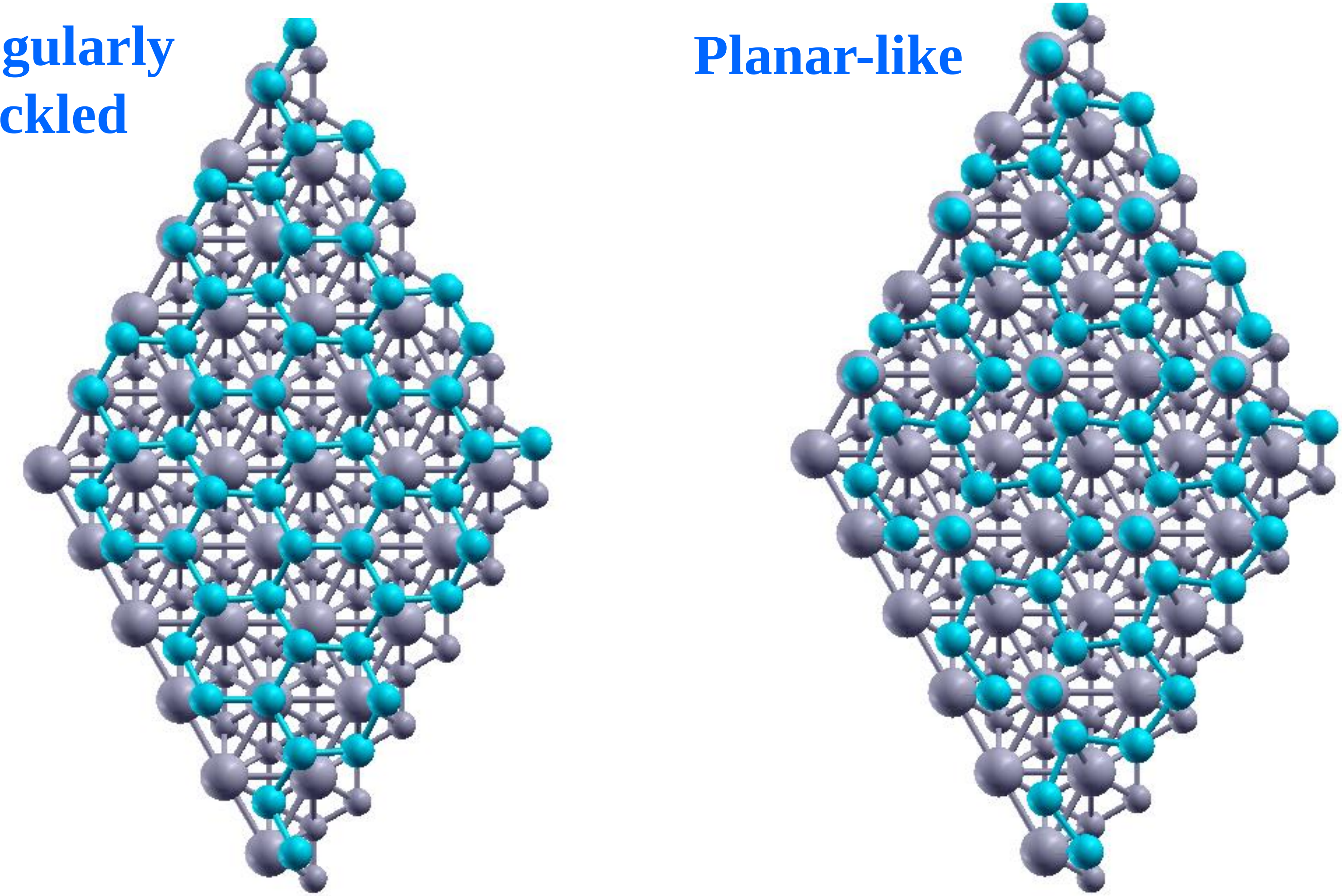

**Regularly buckled**

**Planar-like**

# Optimized structures

## Regularly buckled

$E_{bind}$=1.14 eV/ Si atom

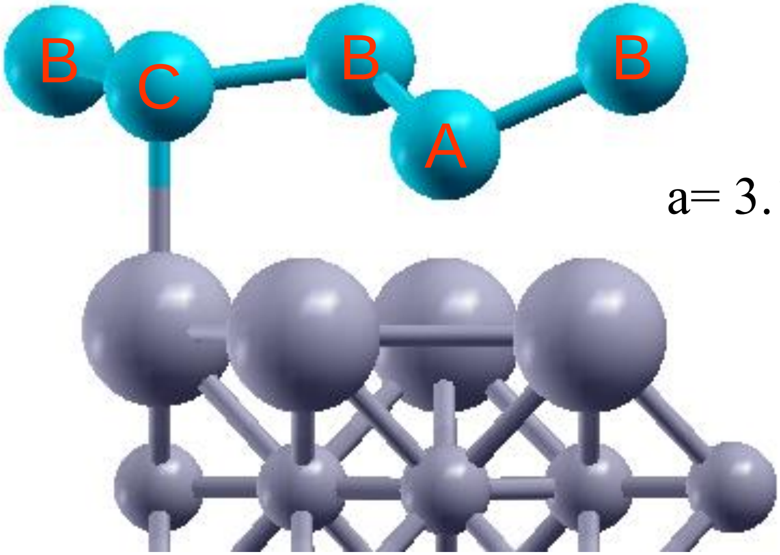

a= 3.187Å

## Planar-like

$E_{bind}$=1.42 eV/Si atom

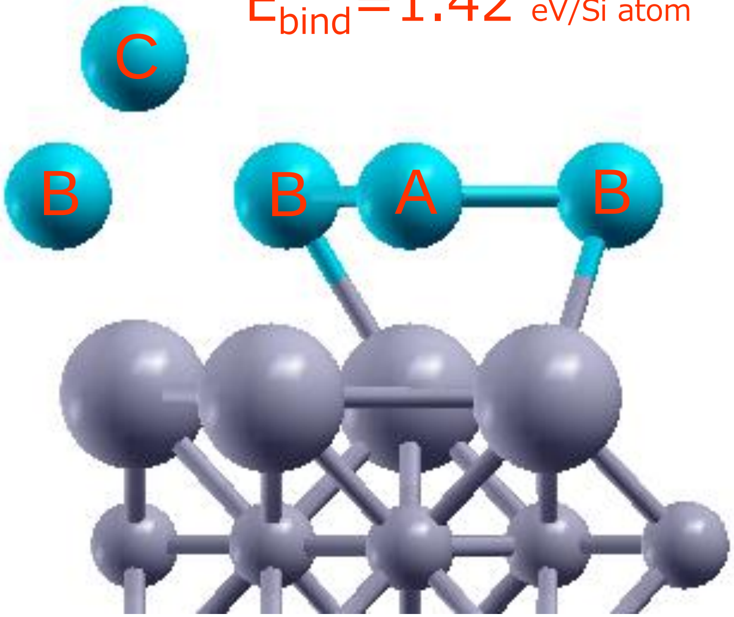

| | A hollow | B bridge | C on-top | A hollow | B bridge | C on-top |
|---|---|---|---|---|---|---|
| Distance from the top Zr layer (Ang.) | 2.105 | 3.043 | 2.749 | 2.328 | 2.331 | 3.911 |
| Distance with neighbor Si atoms (Ang.) | 2.263 | 2.268 | 2.249 | 2.324 | 2.340 | 2.380 |
| Angle with neighbor Si atoms (Deg.) | 104.2 | 110.1 | 118.2 | 120.2 | 113.0 | 80.5 |

# STM image

Expt.

V=100mV

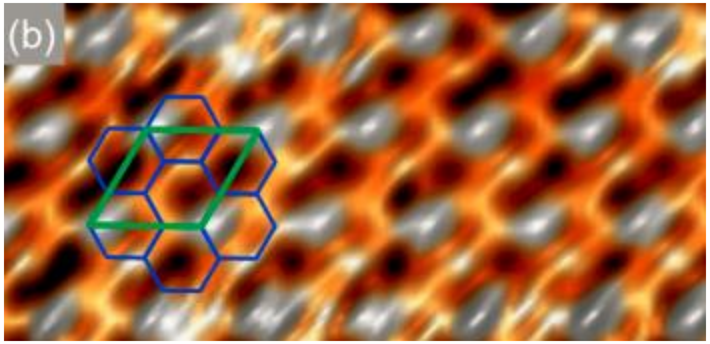

The calculations were performed by the Tersoff-Hamman approximation, and an isovalue of $8x10^{-7}$ e/bohr$^3$ was used for generation of the height profile for both the cases.

**Regularly buckled**

V=+300mV

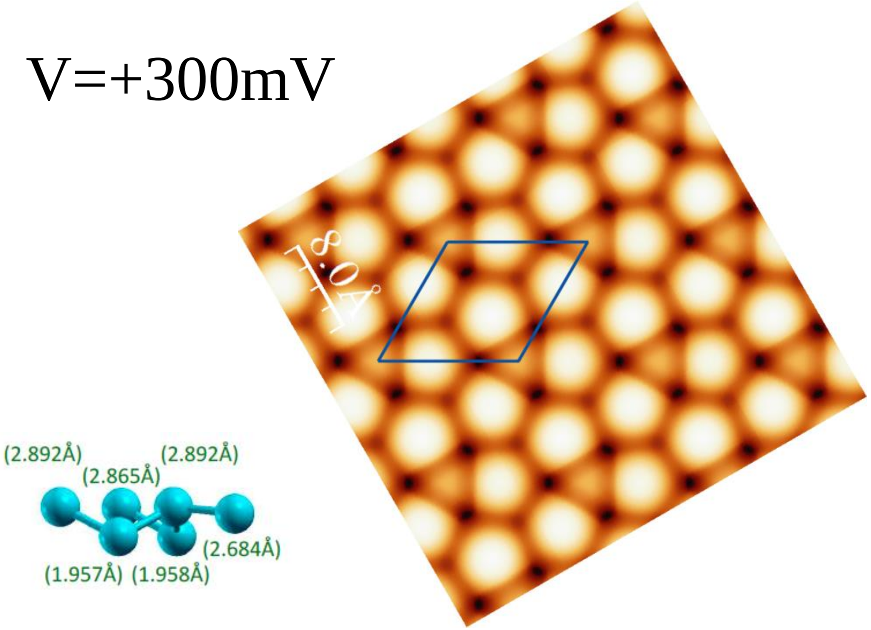

Si$_B$ is blight.

**Planar-like**

V=+300mV

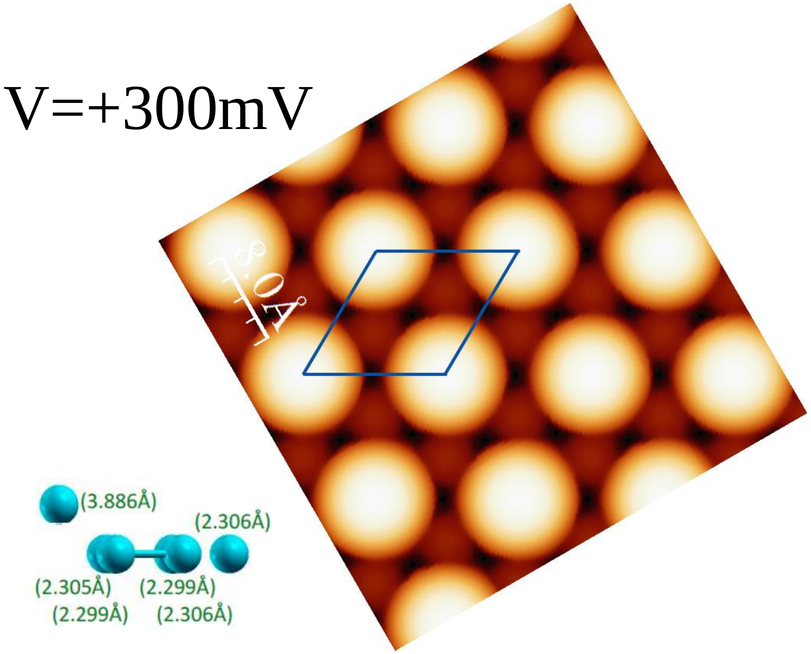

Si$_C$ is blight.

# ARPES and calculated bands

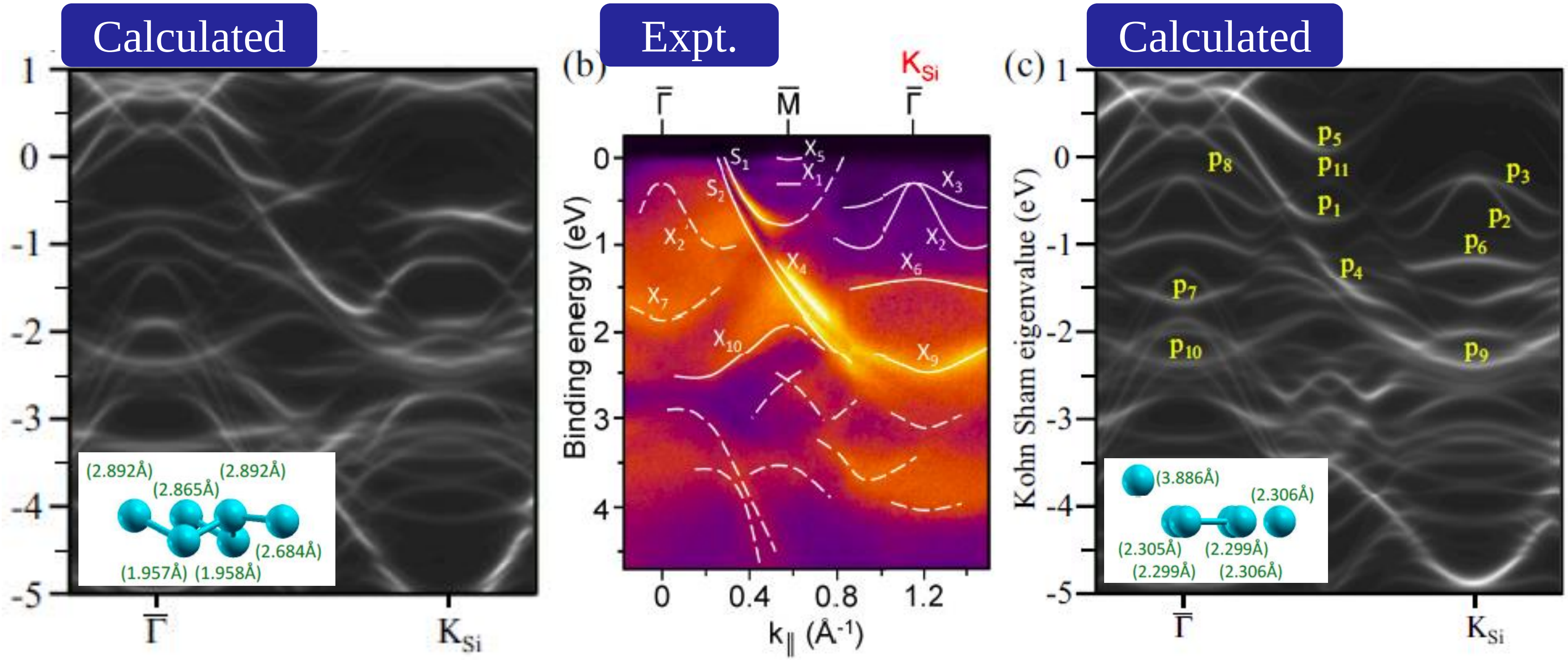

The ARPES intensity spectrum is well reproduced by the band structure of planar-like structure more than that of the buckled like structure, especially for $S_1$, $S_2$, $X_2$ and $X_3$ bands.

C.-C. Lee et al., PRB **90**, 075422 (2014).

# Domain structure of silicene on $ZrB_2$

- Silicene on $ZrB_2$ spontaneously forms a domain (stripe) structure.
- Release of strain might be a reason for that to reduce the areal density of Si.

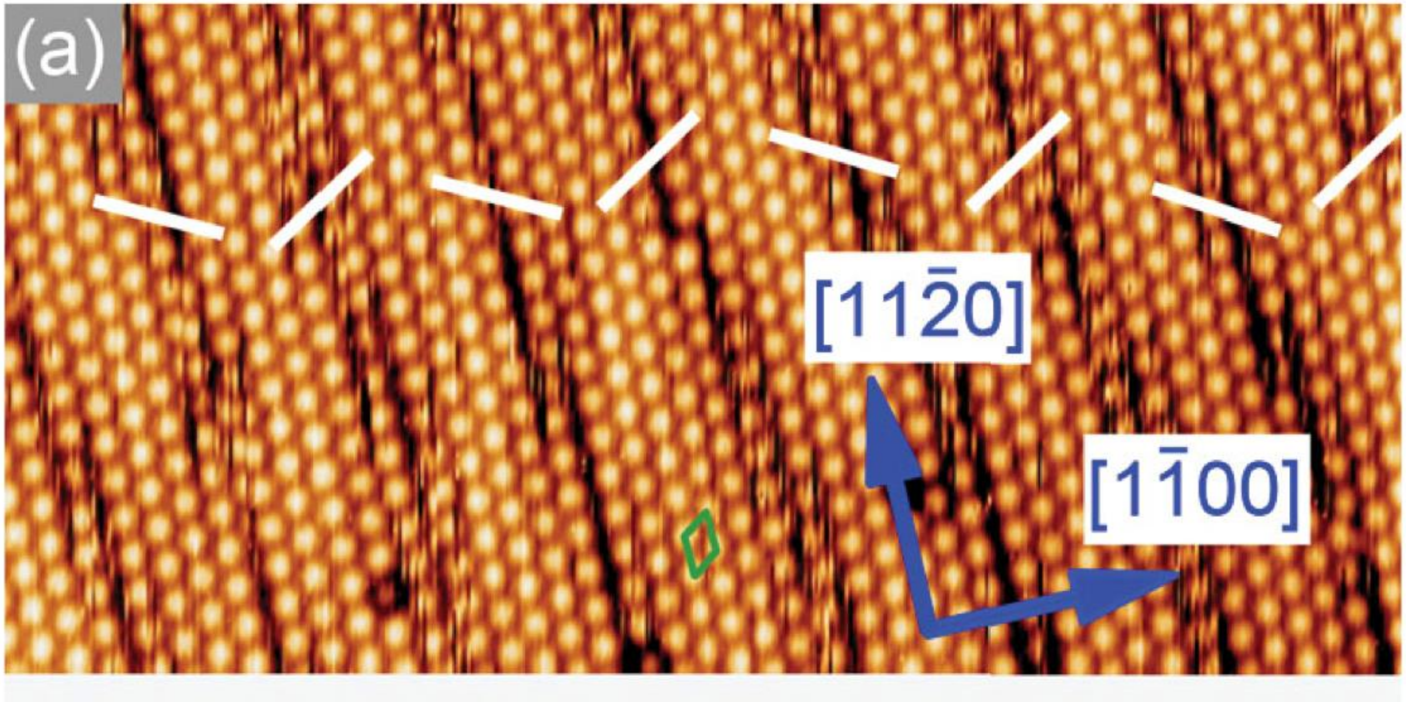

A. Fleurence et al., PRL 108, 245501 (2012).

# Phonon dispersion of silicene on $ZrB_2$

C-.C. Lee et al., Phys. Rev. B 90, 241402 (2014).

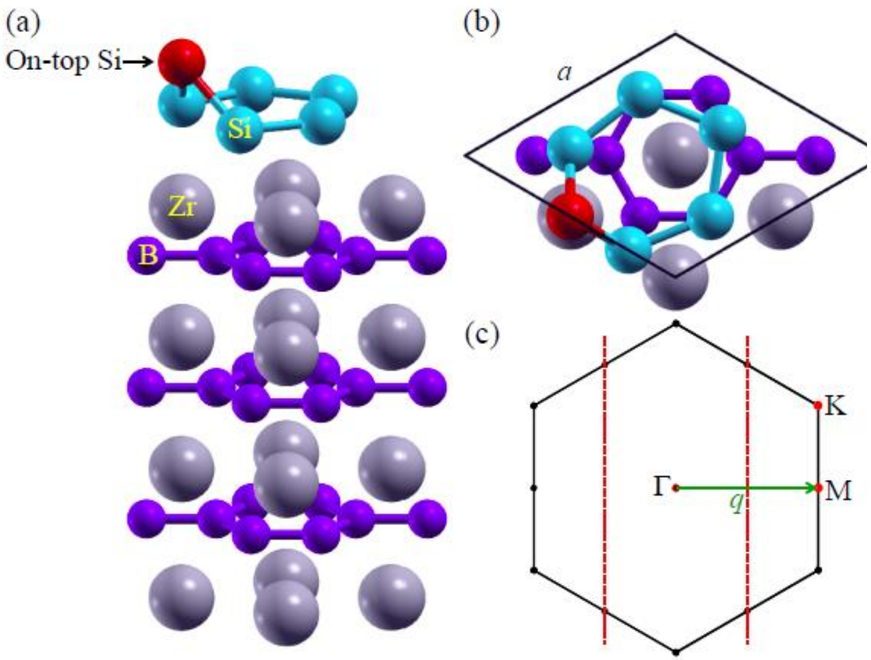

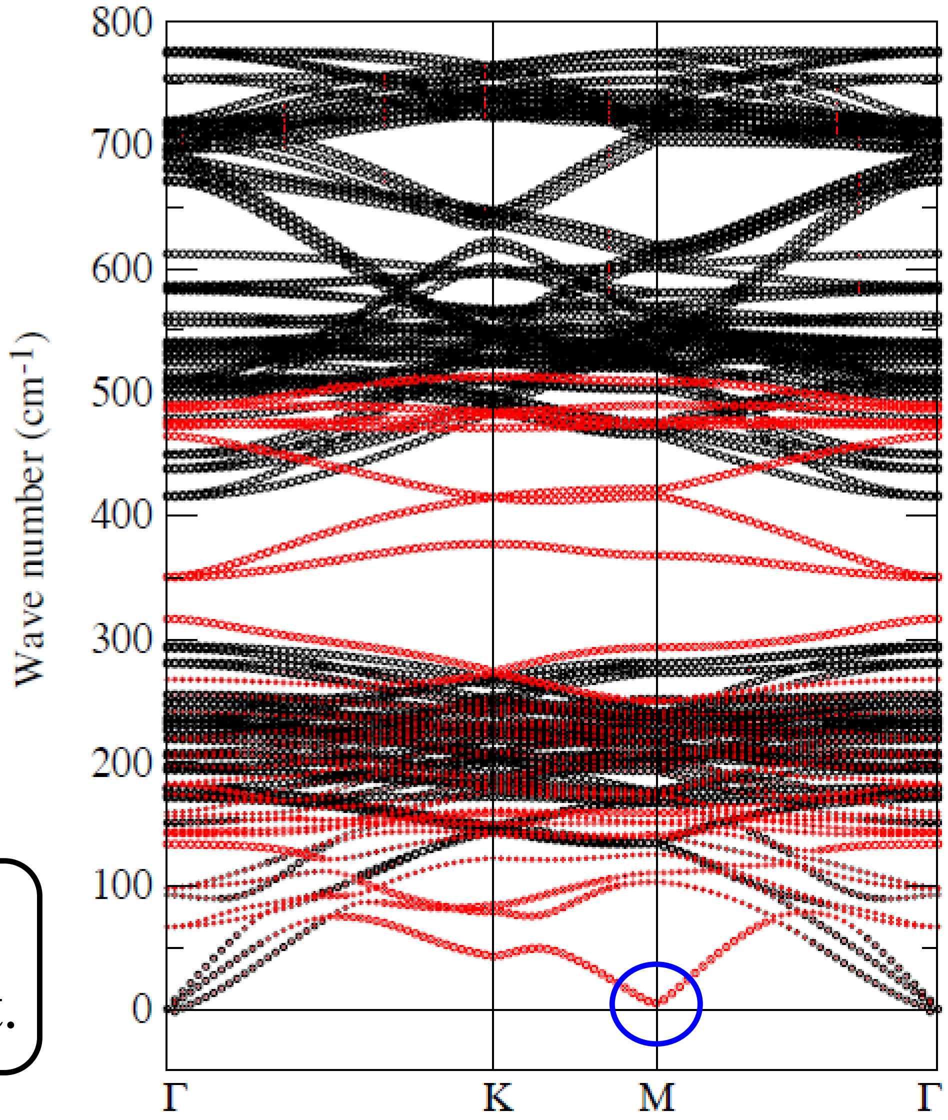

red: silicene black: $ZrB_2$

The softest mode reaches the “zero” frequency at the M point.

# Eigendisplacement at the M-point with zero frequency

All the Si atoms move nearly perpendicular to the red dot line formed by connecting the top Si atoms.

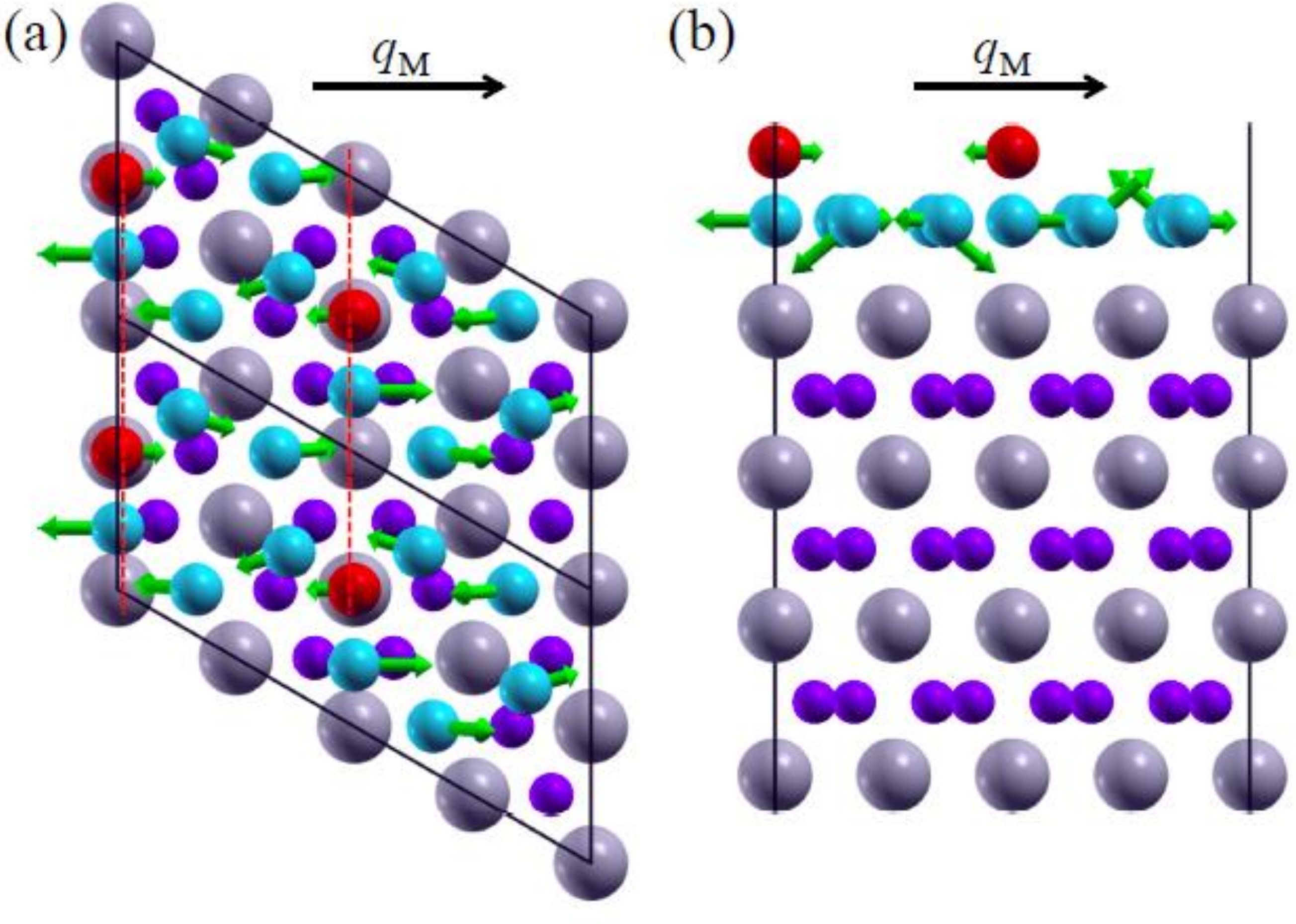

# Avoiding the six M-points with zero frequency

The six M-points can be avoided by changing the BZ as shown below.

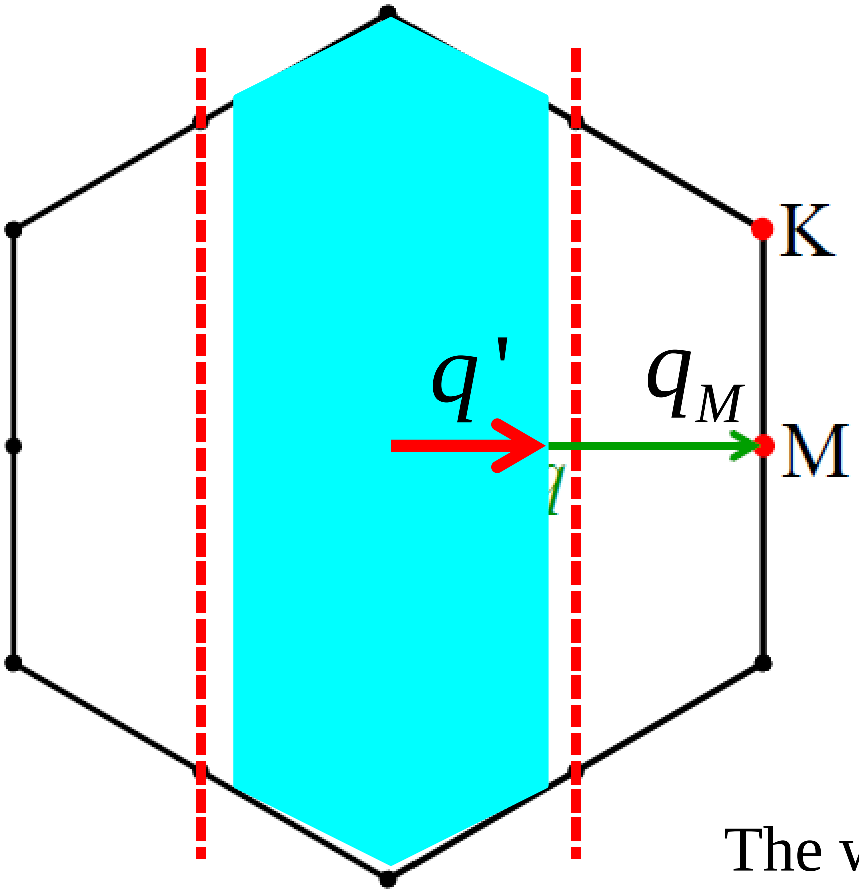

**Condition**

$$\boxed{q' < \frac{q_M}{2}}$$

$$q' \times \frac{\sqrt{3}}{2} a \times N = 2\pi \qquad q_M = \frac{2\pi}{\sqrt{3}}$$

$$\boxed{4 < N}$$

The width $N$ should be larger than 4 to avoid the six M-points.

# Total energy calculations of the domain structures

C-.C. Lee et al., Phys. Rev. B 90, 241402 (2014).

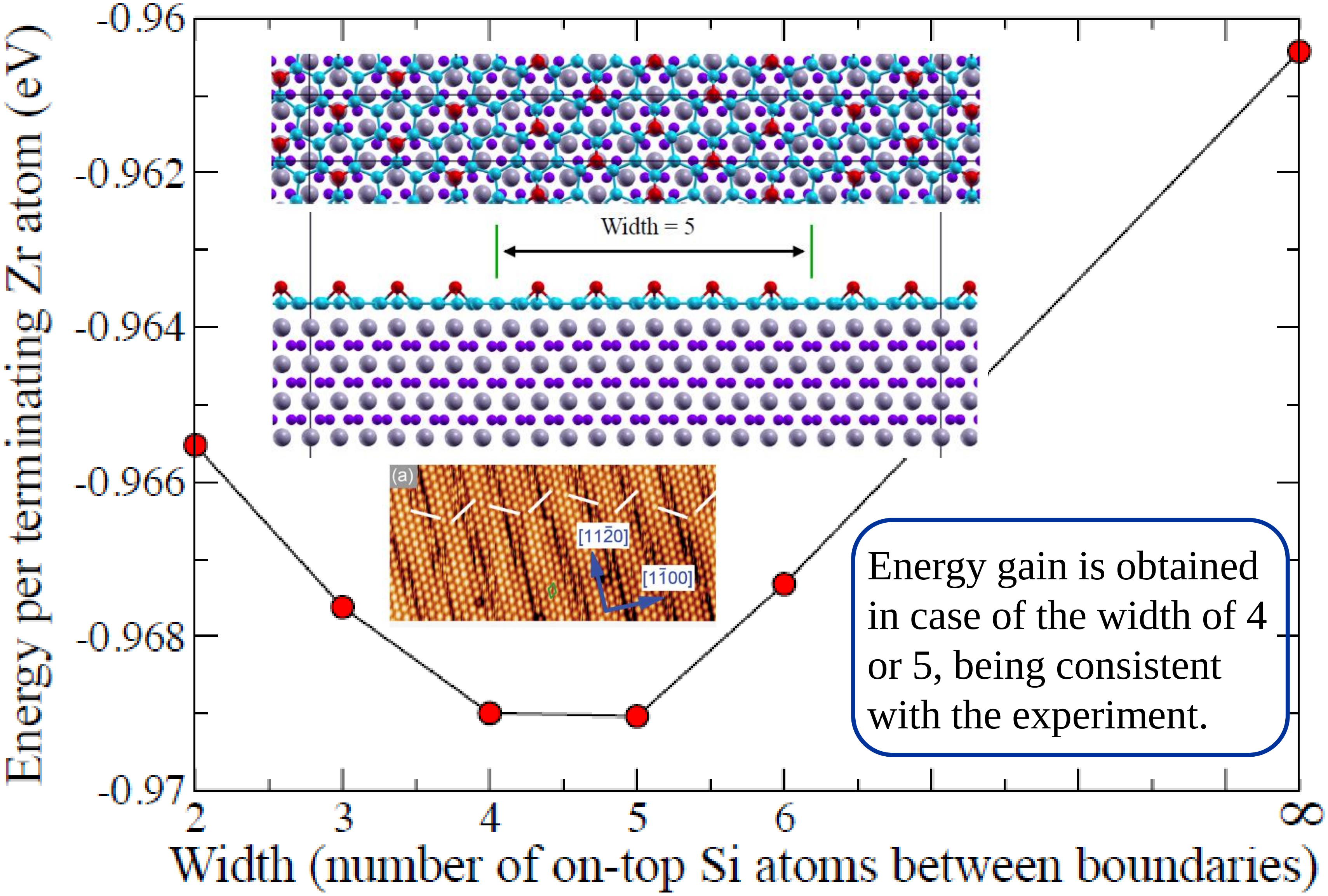

Energy gain is obtained in case of the width of 4 or 5, being consistent with the experiment.

# XPS of Si-2p: Expt. vs. calculations

The XPS data is well compared with the calculated binding energy of planar-like structure.

By the Yoshinobu-lab. in ISSP

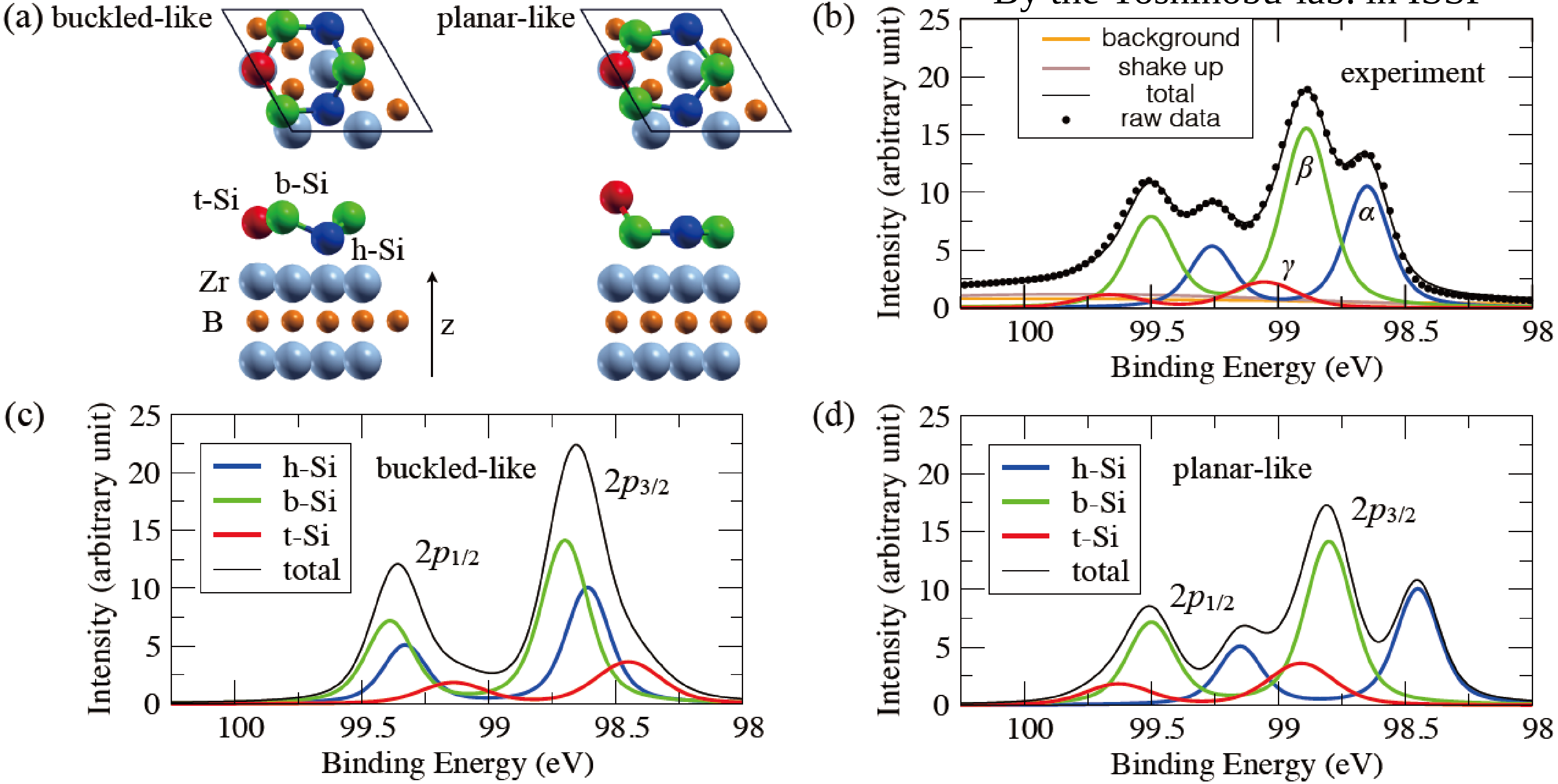

C.-C. Lee et al., PRB 95, 115437 (2017).

# Characterization of structure by expt. and calcs.

In 2012, a regularly-buckled structure was supposed.

The DFT calculations of ARPES, phonon, and XPS strongly support a planar structure.

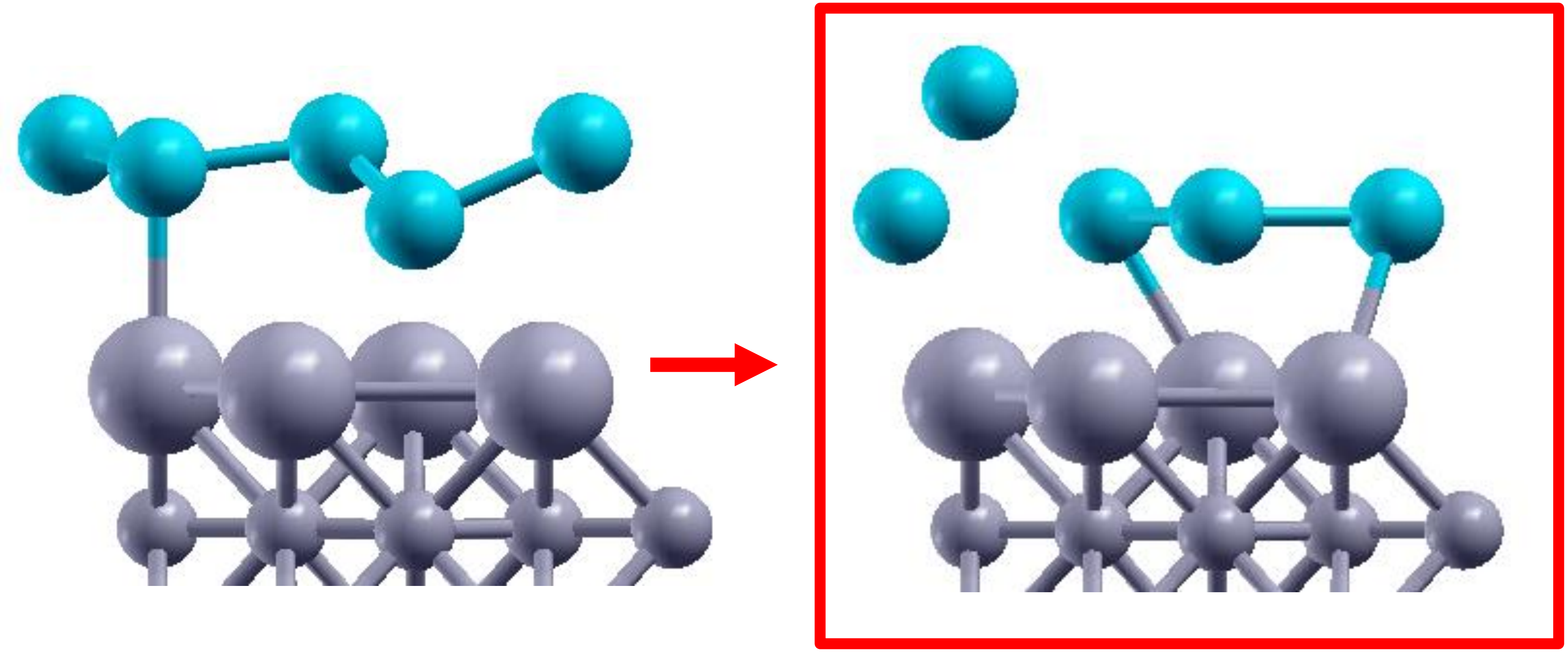

# $\beta_{12}$-Borophene on Ag (111)

In collaboration with the I. Matsuda group in ISSP

Computational model

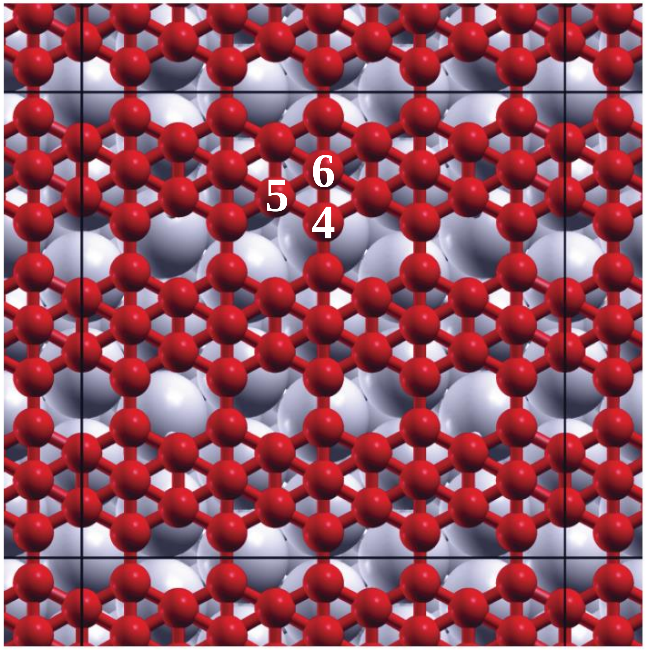

B-1s binding energies

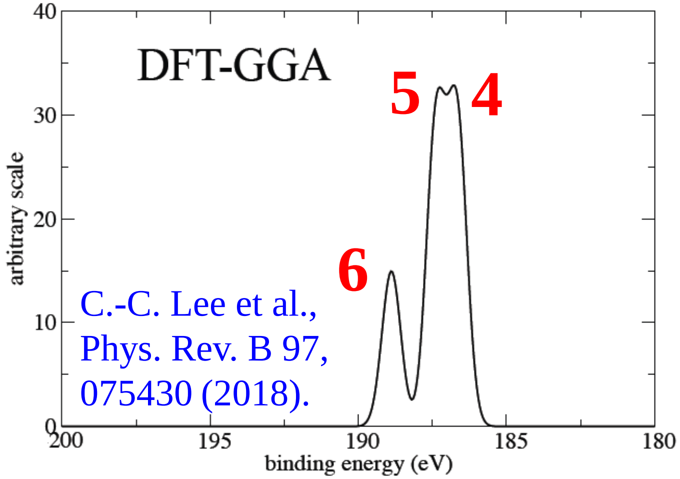

C.-C. Lee et al., Phys. Rev. B 97, 075430 (2018).

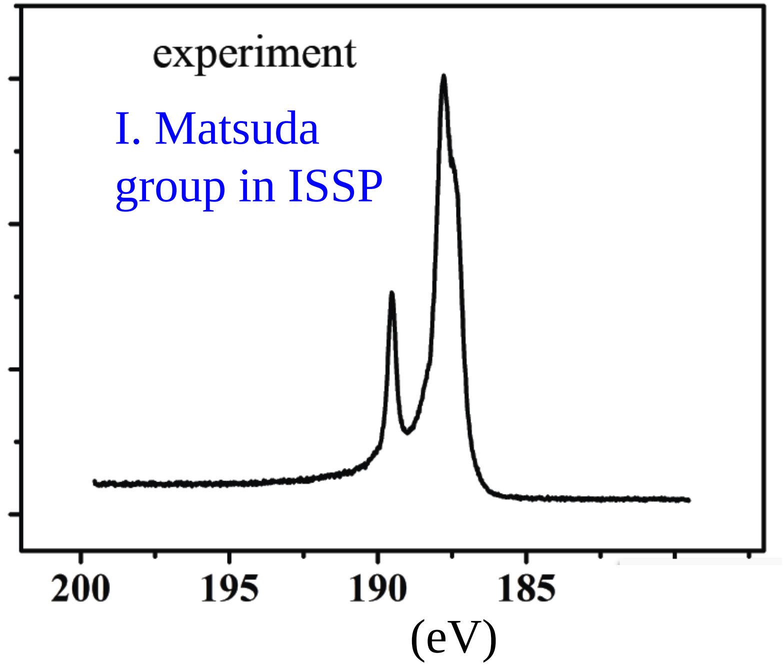

I. Matsuda group in ISSP

STM images from Feng et al, PRB 94, 041408 (3016).

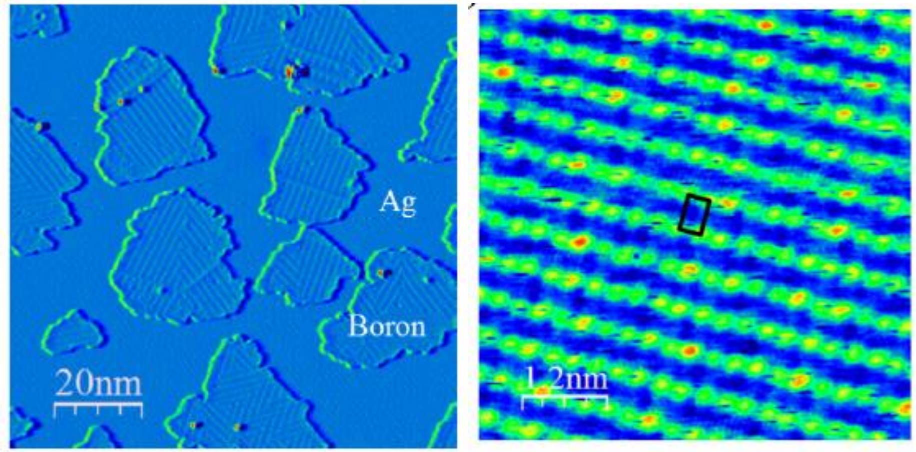

# Bonding states in $\beta_{12}$-borophene

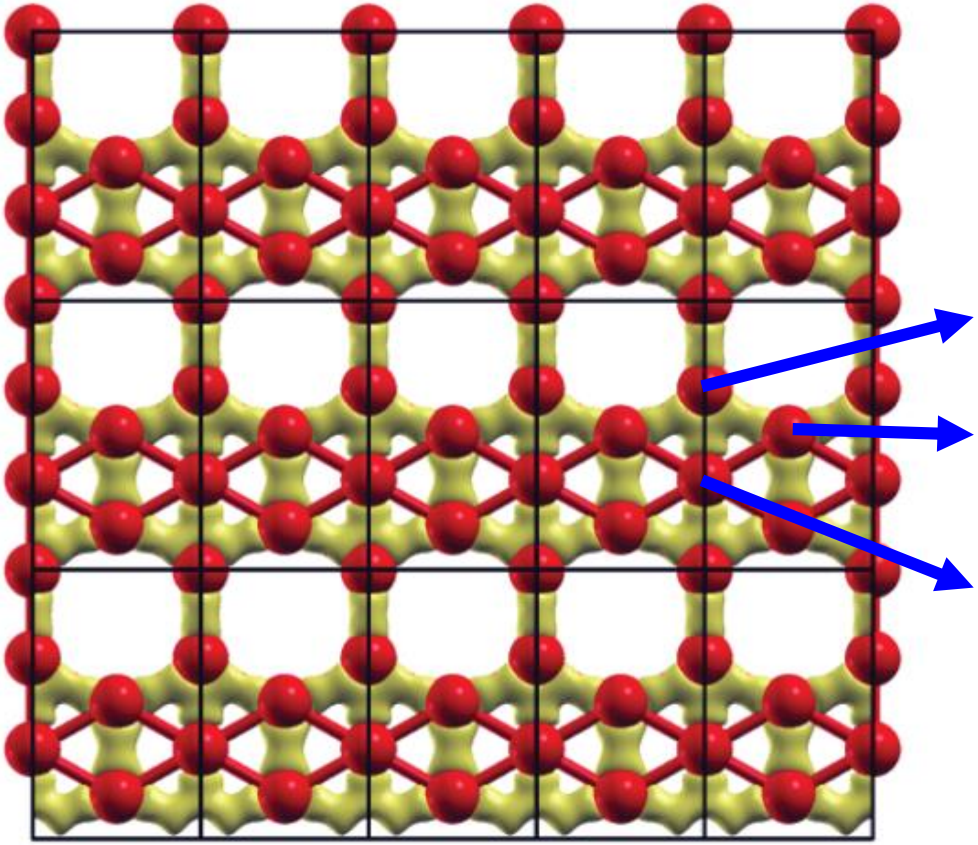

0.125 e/bohr$^3$

| 1s-binding energy (eV) | Coordination number | # of bondings |
|---|---|---|
| 186.228 | 4 | 4 |
| 186.946 | 5 | 3 |
| 188.646 | 6 | 2 |

The number of bondings contradicts to the coordination number.

# Wannier functions in $\beta_{12}$-borophene

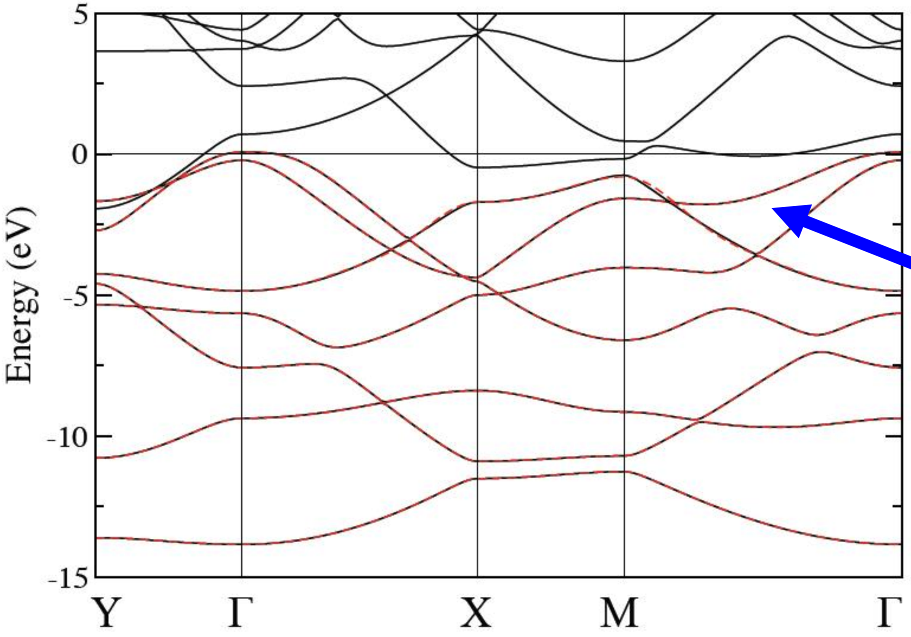

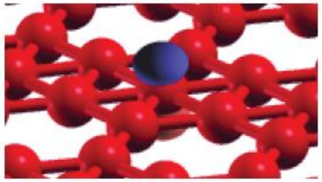

0.1 sqrt(e/bohr³)

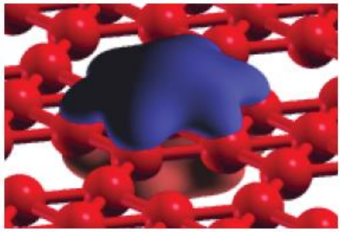

0.05 sqrt(e/bohr³)

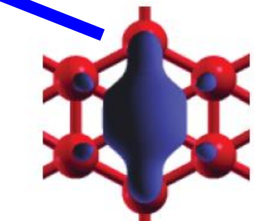

0.07 sqrt(e/bohr³)

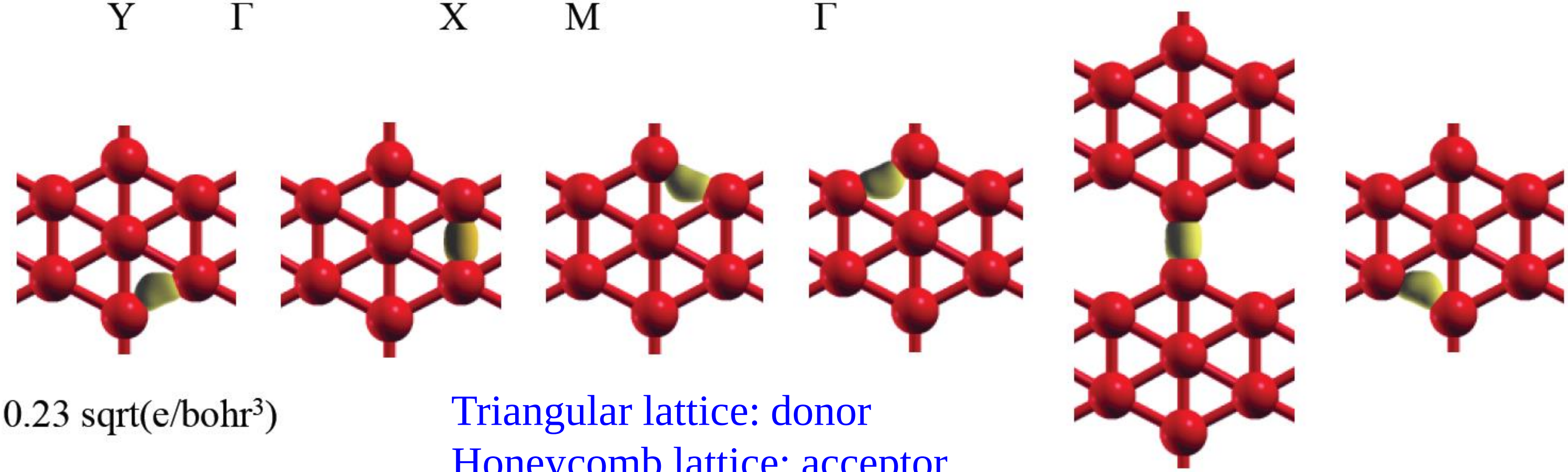

0.23 sqrt(e/bohr³)

Triangular lattice: donor
Honeycomb lattice: acceptor

# Exercise 8: binding energy of C-1s in TiC

1. Perform a calculation for the ground state.

Specify the basis function and pseudopotential of C including the 1s state.

```
Species.Number       3
<Definition.of.Atomic.Species
  Ti  Ti7.0-s3p2d2              Ti_PBE13
  C   C6.0_1s-s3p2d1            C_PBE17_1s
  C1  C6.0_1s_CH-s3p2d1         C_PBE17_1s
Definition.of.Atomic.Species>
```

Input file

https://t-ozaki.issp.u-tokyo.ac.jp/ISS18/input/TiC8-i.dat

2. Perform a calculation for the excited state.

A core hole is introduced in the atom 5.

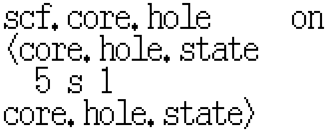

```
scf.core.hole        on
<core.hole.state
  5 s 1
core.hole.state>
```

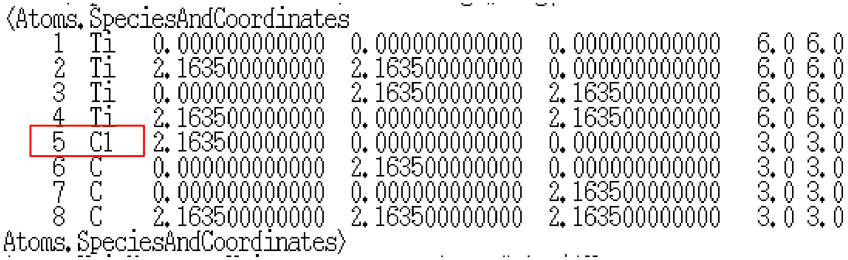

```
<Atoms.SpeciesAndCoordinates
   1  Ti   0.000000000000  0.000000000000  0.000000000000   6.0 6.0
   2  Ti   2.163500000000  2.163500000000  0.000000000000   6.0 6.0
   3  Ti   0.000000000000  2.163500000000  2.163500000000   6.0 6.0
   4  Ti   2.163500000000  0.000000000000  2.163500000000   6.0 6.0
   5  C1   2.163500000000  0.000000000000  0.000000000000   3.0 3.0
   6  C    0.000000000000  2.163500000000  0.000000000000   3.0 3.0
   7  C    0.000000000000  0.000000000000  2.163500000000   3.0 3.0
   8  C    2.163500000000  2.163500000000  2.163500000000   3.0 3.0
Atoms.SpeciesAndCoordinates>
```

Specify a restart file for $\rho_i$, and apply the exact Coulomb cutoff method.

```
scf.restart                    on
scf.restart.filename           TiC8
scf.coulomb.cutoff             on
```

Input file

https://t-ozaki.issp.u-tokyo.ac.jp/ISS18/input/TiC8-f.dat

3. Calculate the absolute binding energy by either Eb = Ef – Ei or Ef – Ei + μ.

# Relevant keywords

The other relevant keywords for the core hole calculation are given below:

```
scf.restart                 on
scf.restart.filename       TiN8
scf.coulomb.cutoff          on
scf.core.hole               on

<core.hole.state
  5 s 1
core.hole.state>

scf.system.charge           1.0      # default=0.0
```

In the final state, the restart files, generated by the initial state calculation, has to be read. The relevant keywords are scf.restart and scf.restart.filename. Also, the non-periodic charge density is treated by the exact Coulomb cutoff method, specified by the keyword: scf.coulomb.cutoff. The core hole is introduced by the keywords: scf.core.hole and core.hole.state. Also, due to the creation of core hole, the system is charged up by the keyword: scf.system.charge.

# Specification of Keyword “core.hole.state”

The orbital

```
<core.hole.state
   5 s 1
core.hole.state>
```

The first: atomic index
The second: target l-channel (s, p, d, or f)
The third: orbital index (1 to 4l+2)

## Collinear case

| | | | | | | | |
|---|---|---|---|---|---|---|---|
| s | 1: s↑ | 2: s↓ | | | | | |
| p | 1: $p_x$↑ | 2: $p_y$↑ | 3:$p_z$↑ | 4: $p_x$↓ | 5: $p_y$↓ | 6:$p_z$↓ | |
| d | 1: $d_{3z2-r2}$↑ | 2: $d_{x2-y2}$↑ | 3:$d_{xy}$↑ | 4: $d_{xz}$↑ | 5: $d_{yz}$↑ | | |
| | 6: $d_{3z2-r2}$↓ | 7: $d_{x2-y2}$↓ | 8:$d_{xy}$↓ | 9: $d_{xz}$↓ | 10: $d_{yz}$↓ | | |
| f | 1: $f_{5z2-3r2}$↑ | 2: $f_{5xz2-xr2}$↑ | 3: $f_{5yz2-yr2}$↑ | 4: $f_{zx2-zy2}$↑ | 5: $f_{xyz}$↑ | 6: $f_{x3-3xy2}$↑ | 7: $f_{3yx2-y3}$↑ |
| | 8: $f_{5z2-3r2}$↓ | 9: $f_{5xz2-xr2}$↓ | 10: $f_{5yz2-yr2}$↓ | 11: $f_{5yz2-yr2}$↓ | 12: $f_{5yz2-yr2}$↓ | 13: $f_{5yz2-yr2}$↓ | 14: $f_{5yz2-yr2}$↓ |

## Non-collinear case

| | | | | | | | | |
|---|---|---|---|---|---|---|---|---|
| s | 1: J = 1/2<br>M = 1/2 | 2: J = 1/2<br>M = -1/2 | | | | | | |
| p | 1: J = 3/2<br>M = 3/2 | 2: J = 3/2<br>M = 1/2 | 3: J = 3/2<br>M = -1/2 | 4: J = 3/2<br>M = -3/2 | 5: J = 1/2<br>M = 1/2 | 6: J = 1/2<br>M = -1/2 | | |
| d | 1: J = 5/2<br>M = 5/2 | 2: J = 5/2<br>M = 3/2 | 3: J = 5/2<br>M = 1/2 | 4: J = 5/2<br>M = -1/2 | 5: J = 5/2<br>M = -3/2 | 6: J = 5/2<br>M = -5/2 | | |
| | | 7: J = 3/2<br>M = 3/2 | 8: J = 3/2<br>M = 1/2 | 9: J = 3/2<br>M = -1/2 | 10: J = 3/2<br>M = -3/2 | | | |
| f | 1: J = 7/2<br>M = 7/2 | 2: J = 7/2<br>M = 5/2 | 3: J = 7/2<br>M = 3/2 | 4: J = 7/2<br>M = 1/2 | 5: J = 7/2<br>M = -1/2 | 6: J = 7/2<br>M = -3/2 | 7: J = 7/2<br>M = -5/2 | 8: J = 7/2<br>M = -7/2 |
| | | 9: J = 5/2<br>M = 5/2 | 10: J = 5/2<br>M = 3/2 | 11: J = 5/2<br>M = 1/2 | 12: J = 5/2<br>M = -1/2 | 13: J = 5/2<br>M = -3/2 | 14: J = 5/2<br>M = -5/2 | |

# Database (2017) of optimized VPS and PAO

For B, C, N, O, Si, Pt, pseudopotentials and basis functions are available to calculate binding energies of core levels.

https://t-ozaki.issp.u-tokyo.ac.jp/vps_pao2017/

The functionality will be released in OpenMX Ver. 3.9.

# Outlook

The method based on a penalty functional and an exact Coulomb cutoff enable us to calculate absolute binding energies of core levels in solids with the following features:

- applicable to insulators and metals
- accessible to absolute binding energies
- screening of core and valence electrons on the same footing
- SCF treatment of spin-orbit coupling
- exchange interaction between core and valence states
- geometry optimization with a core hole state

By applying the method for silicene on $ZrB_2$, we have obtained a conclusive agreement between the experiments and calculations.

TO and C.-C. Lee, Phys. Rev. Lett. 118, 026401 (2017).
C.-C. Lee et al., Phys. Rev. B 95, 115437 (2017).
C.-C. Lee et al., Phys. Rev. B 97, 075430 (2018).